

**Identification of genetic risk variants for atherosclerosis using
oxidative stress assays in vascular smooth muscle cells and
bioinformatic approaches**

*Identifikation genetischer Risikovarianten für Artherosklerose via
oxidativem Stress Assay in glatten Muskulaturzellen und
bioinformatische Ansätze*

Masterarbeit

verfasst am
Institut für Kardiogenetik

im Rahmen des Studiengangs
Molecular Life Science
der Universität zu Lübeck

vorgelegt von
Torben Falk

ausgegeben und betreut von
Prof. Dr. Jeanette Erdmann

mit Unterstützung von
Dr. Tobias Reinberger

Lübeck, den 21. Juli 2022

Eidesstattliche Erklärung

Ich erkläre hiermit an Eides statt, dass ich diese Arbeit selbständig verfasst und keine anderen als die angegebenen Quellen und Hilfsmittel benutzt habe.

Torben Falk

Zusammenfassung

Ich muss das Ding wohl irgendwann auch noch in Deutsch schreiben...

Abstract

Placeholder, this is more or less what I am doing:

I am currently writing my Master thesis at the university of Lübeck at the [Institute for Cardiogenetics](#) on the topic of “Identification of genetic risk variants for atherosclerosis using oxidative stress assays in vascular smooth muscle cells and bioinformatic approaches”:

Coronary artery disease (CAD) describes the arterial build-up of fatty deposits to a point where the blood supply to the heart gets interrupted. It is one of the major causes of death worldwide. Risk factors for CAD are typical lifestyle factors like smoking or physical inactivity, but also include hereditary factors ([cdcCoronaryArteryDisease2021](#); [CoronaryHeartDisease2018](#)). These can provide access to the molecular pathology of the disease. One amazing resource for studying these interactions are genome wide association studies (GWAS). Unfortunately, GWAS are just the first step in a longer journey of establishing causal loci to gene links, uncovering the molecular basis of disease, and implementing tools for clinical risk prediction. A plethora of follow-up analyses (postGWAS) can and need to be performed ([lichouFunctionalStudiesGWAS2020a](#)).

We hypothesize that oxidative stress in smooth muscle cells plays a role in stability of atherosclerotic plaques. For this reason, I am cultivating and differentiating primary human smooth muscle cells and characterizing them using oxidative stress assay, qPCR, seahorse assay & immunofluorescence (IF).

Additionally, I am working with GWAS data on CAD ([aragamDiscoverySystematicCharacterization2021a](#)). Curating further publicly available data that can be used for bioinformatic follow-up analyses like the enrichment for involved tissues. Further, I am using the data to build a web application that allows co-visualization and visual exploration.

Acknowledgements

Daaanke an alle!

Contents

1	Introduction	1
1.1	Coronary artery disease	1
1.2	Muscle Cells in CAD	1
1.3	Transforming Growth Factor beta ($TGF\beta$) Signaling	2
1.4	PDGF Signaling	2
1.5	GWAS	3
1.6	Complementary High Through Put Methods	5
1.7	Aim of the thesis	6
2	Material	8
2.1	Manufactors	8
2.2	Antibodies	9
2.3	Celllines	9
2.4	Primer	9
2.5	Chemicals	10
2.6	Media, Supplements	11
2.7	Solutions	11
2.8	Kits	11
2.9	Consumables	11
2.10	Devices	12
2.11	Programs & Modules	13
2.12	Public Data	14
3	Methods	15
3.1	Cultivation and differentiation of HAoSMCs	15
3.2	mRNA Quantification	16
3.3	Energy Profiling	18
3.4	Oxidative Stress Assay	20
3.5	Immunoflourescence	20
3.6	Curation of Data for postGWAS Analyses	21
3.7	Visualization of GWAS data	22
3.8	Enrichment analysis	23
4	Results	25
4.1	Differentitaion	25
4.2	Evaluation of oxidative Stress	27
4.3	Database and GWAS Visualizer	28

4.4	Enrichment analysis	28
5	Discussion	37
6	Conclusion & Outlook	41

1

Introduction

1.1 Coronary artery disease

Coronary artery disease (CAD) is among the leading causes of death in the (western) world wide, being prevalent in about 6.7 % of US-american adults and killing more than 350'000 people in the USA in 2019 (Disease Control and Prevention, [2022](#); Fryar, [2012](#)). Its most common complication is myocardial infarction (MI), which usually manifests by chest pain (angina) and can cause serious damage to the heart muscle. CAD is characterised by the build up of fatty plaques in the arteries leading to the heart. This process, also called atherosclerosis, can interrupt the blood supply of the heart (National Health Service, [24 Oct 2017, 4:45 p.m.](#)). Next to common and well known life-style factors like tobacco use or physical inactivity, CAD risk additionally has an hereditary component (Task Force Members et al., [2013](#)).

1.2 Muscle Cells in CAD

The lumen of a typical blood vessel is surrounded by three distinct layers. The outer adventitia is rich in connective tissue, shapes the vessel and wraps the media. The media contains vascular smooth muscle cells (VSMCs). VSMCs of the media are required to mediate vasodilation and vasoconstriction according to signaled requirements. The innerlayer consists of endothelial cells that define the lumen of the vessel (Tucker, Arora, and Mahajan, [2022](#); Yap et al., [2021](#)).

For the longest time the role of VSMCs in the development and progression of atherosclerosis has been underestimated and over simplified. They have simply either been considered to be either promoting of arterogenesis or beneficial for plaque stability. Only with the emergence of novel and exciting technologies like single cell transcriptomics and lineage tracking, this view is changing to a more differentiated one (Grootaert and Bennett, [2021](#); Yap et al., [2021](#)). The study of VSMCs in atherosclerosis is rapidly evolving and the underlying model adjusted accordingly. The black and white model of VSMCs in atherosclerosis existing either as a differentiated (contractile) phenotype or as a dedifferentiated (synthetic) phenotype, is making place for a model that considers a diverse set of dedifferentiated phenotypes (Grootaert and Bennett, [2021](#); Yap et al., [2021](#)). During the phenotypic switch describes the down regulation of contractile markers and the rising of bouquet of dif-

ferent phenotypes which can be found in the fibrous cap and plaque core (Grootaert and Bennett, 2021). The number as well as their impact on disease progression are still subject of intensive research.

Two external stimuli that seem to play central roles as cytokines determining the fate of VSMCs in arterogenesis are $\text{TGF}\beta$ & platelet-derived growth factor-BB (PDGF-BB).

1.3 $\text{TGF}\beta$ Signaling

$\text{TGF}\beta$ Signaling in General

$\text{TGF}\beta$ is a summarizing term for a superfamily of cytokines, the most prominent of which is $\text{TGF}\beta 1$. After secretion and activation, the active $\text{TGF}\beta$ dimer binds to a heteromeric receptor complex, that mainly implements its signaling via Smad transcription factors. The effects of $\text{TGF}\beta$ is highly dependant on the cell type and can even be pleiotropic for cells of the same type. The most prominent function of $\text{TGF}\beta$ is its role in antiinflammatory regulation of immune cells (Goumans and Dijke, 2018; Batlle and Massagué, 2019).

$\text{TGF}\beta$ Signaling VSMCs & atherosclerosis

In the context of VSMCs, $\text{TGF}\beta$ promotes proliferation and hypertrophy. Further it promotes VSMC differentiation, via elevation of contractile gene expression as well as the down regulation of Kruppel-like factor 4 (KLF4) (Davis-Dusenbery et al., 2011), a transcription factor (TF) prominent for its application in inducing pluripotency (Takahashi et al., 2007) that is also required for phenotype switching. This way hindering (Davis-Dusenbery et al., 2011) or potentially reversing phenotype switching (Pan et al., 2020).

1.4 PDGF Signaling

PDGF Signaling in General

Five different PDGF isoforms have been identified that form as dimeric combination of four distinct polypeptide chains (PDGF-AA, PDGF-AB, PDGF-BB, PDGF-CC & PDGF-DD). All five bind to tyrosine kinase receptors (Platelet-derived growth factor receptor (PDGFR) α & PDGFR β). Upon activation, the receptor dimerize, allowing autophosphorylation which activates the kinase domain and creates binding sites for signaling molecules. The active receptor is involved in a plethora of prominent messanging pathways like the mitogen activated protein (MAP)-kinase pathway, phosphatidylinositol 3'-kinase (PI3K)-signaling or signal transducers and activators of transcription (STAT)-signaling. All these pathways are ultimately involved in the promotion of cellular proliferation, survival and migration (Chen, Chen, and He, 2013; Heldin, 2013; Hu and Huang, 2015).

PDGF-B seems to be the majorily expressed isoform of PDGF in endothelial cells (Andrae, Gallini, and Betsholtz, 2008; Heldin, 2013) and acts as a paracrine activator for VSMCs and other mesenchymal cells (Heldin, 2013). Signaling via PDGF-BB and the PDGFR β plays an important role in development of multiple tissues, e.g. in the development of the cardio vascular system (Levéen et al., 1994). After completed development, PDGF-BB picks up an important role in wound healing (Robson et al., 1992). The role of

PDGFR β signaling in pathologic processes like cancer or cardio vascular disease has been a subject of extensive study for decades (Heldin, 2013; Raines, 2004).

PDGF Signaling in VSMCs & atherosclerosis

In the context of VSMCs, PDGF-BB was shown to increase KLF4 levels, which results in upregulation of mesenchymal markers as well as the loss of contractile markers. Ultimately serving as an external stimulus for proliferation and phenotype switching (Yap et al., 2021).

Similarly to the overall role of VSMCs in atherosclerosis, the role of PDGF-BB is still subject of extensive study. All PDGF isoforms are abundantly found in atherosclerotic cell walls and PDGFR expression is elevated in affected vessels (Hu and Huang, 2015). For a long time PDGF signaling and inflammation has been assumed to be disease promoting (Andrae, Gallini, and Betsholtz, 2008; Chen, Chen, and He, 2013; He et al., 2015; Hu and Huang, 2015) and in 2015 He et al. (2015) showed that PDGFR β signaling in mouse model leads to inflammation and increased plaque formation. In contrast to this consensus, Newman et al. (2021) were recently able to demonstrate, that sustained signaling via PDGFR β is required for VSMC involvement. They further observed, in mouse model, that lack of VSMC involvement can be temporarily compensated by non-VSMC-derived cells, but long term leads to instability of atherosclerotic lesions.

ROS in PDGF Signaling

reactive oxygen species (ROS) is a broad term for a class highly reactive molecules derived from elemental oxygen (O_2). They are traditionally infamous for the damage they can do to proteins and nucleic acids when not kept in check, potentially causing irreparable damage leading to cell death. Recently this perception has been shifting, and specifically hydrogen peroxide (H_2O_2) and superoxide anion radical ($O_2^{\cdot -}$), are being recognized for their role in cellular signaling (Sies and Jones, 2020).

Human cells contain dozens of enzymes, which are capable of generating ROS and enzymatically maintain a steady redox state (Sies and Jones, 2020). H_2O_2 and $O_2^{\cdot -}$ serve as important second messengers for processes such as () or repair of vascular lesions (Andrae, Gallini, and Betsholtz, 2008). Interestingly, the generation of ROS as a second messenger also gets triggered by stimulation with PDGF-BB (Sundaresan et al., 1995; Bouzigues et al., 2014).

1.5 GWAS

The hereditary components of disease onset and progression can provide access to the molecular pathology of the disease.

GWAS

An amazing resource for getting a first glance into these interactions are genome wide association study (GWAS), a method that allows for the identification of genetic variants associated with a phenotype.

While GWAS were initially an extraordinary endeavour, requiring the evaluation of hundreds or thousands of participants, they have gotten a lot more accessible with the availability

of genetic data from public biobanks. After profiling the cohort on a genomic level (usually via micro arrays but WGS is probably the future) and phenotypically, the collected data needs to go through several steps of quality control, e.g. for the removal of rare variants, miss matched phenotypes, etc. Afterwards variants which were not directly analyzed can be inferred from a reference. The final step of the initial analysis is the statistical model, where a regression model is used to test for association of all variants with the phenotype in question. It is crucial to be completely aware of potential biases, that might be introduced in this process (mainly in the data collection part), some of which, like age, sex and ancestry can and need to be included as covariates in the used model (Uffelmann et al., 2021; Flint, 2013).

The model will output a list of p-values, effect sizes (and their direction) for all tested variants. A GWAS is the first important step in determining causal variants for disease and therefore a first glimpse into the molecular biology of the observed phenotype (Uffelmann et al., 2021).

Post GWAS

Unfortunately, GWAS are just the first step in a longer journey of establishing causal loci to gene links, uncovering the molecular basis of disease, and implementing tools for clinical risk prediction. A plethora of follow up analyses (postGWAS) can and need to be performed to determine a set of credible variants and to assess their molecular mechanism.

The first important follow-up, that is usually done immediately, is so called fine-mapping. Due to the complex linkage structure of variants in the human genome (which is also utilized for the inference of not studied variants), identified loci in GWAS usually do not contain a single significant variant, but are made up of a potentially large set of linked variants. Fine-mapping describes the process of identifying the actually causal variant in this mess. Multiple very sophisticated statistical methods have been developed, the most popular of which is bayesian modelling which yields variant specific PIPs that form a credible set of potentially causal variants. It is important to remember, that fine-mapping is not a solved problem, available methods are continuously improving and will most likely keep getting more complex with increasing complexity of the studied phenotypes. Further fine-mapping is a solely statistical approach which will never be able to determine causality (Schaid, Chen, and Larson, 2018; Uffelmann et al., 2021)!

While fine-mapping is an additionally essential step, the identification of likely causal variants, still grants only limited direct information on their effect and into the molecular basics of the analyzed phenotype. Variants still require mapping to impacted genes, associated pathways and relevant tissues to get a glance of the complete image. For these steps Unfortunately no standard protocols exist and the procedure highly depends on the genomic context of the variant. Coding variants are and offer themselves to be immediately studied on a protein level, while non-coding variants are greatly benefited from the consultation of more high throughput data in the form of e.g. eQTLs (Uffelmann et al., 2021).

Finally, all the previous results can and need to be taken back to the wet lab, to verify and extend the models derived from statistical models. Utilizing all the recent great advances of molecular and cellular biology, such as the development of increasingly comprehensive *in vitro* models as well and their evaluation via methods like CRISPR gene-editing (Lichou and Trynka, 2020).

1.6 Complementary High Through Put Methods

The development of high through put methods as well as the great increase in computing power over the last few years have spawned a plethora of incredible datasets that all ready have been and can be further utilized for postGWAS analyses. A short overview of some definitions and methods mentioned in this thesis can be found in the following paragraphs:

Linkage Disequilibrium

Linkage disequilibrium is a parameter from populations genetics that describes the non-random association of two or more alleles. The LD is often quantified using the correlation coefficient r^2 (Slatkin, 2008).

$$D_{AB} = p_{AB} - p_A p_B$$

$$r^2 = \frac{D_{AB}^2}{p_A(1 - p_A) \times p_B(1 - p_B)}$$

Where p_A and p_B is the frequency of the alleles A and B respectively. p_{AB} is the frequency of the AB haplotype.

The linkage disequilibrium (LD) becomes important in the context of GWAS because identified SNPs often do not occur in isolation, but a network of linked and significant variants can span large haplotype blocks in the genome (Slatkin, 2008).

Locus To Gene Scores

Problems of interpretation of GWAS data are already described in section 1.5. Link to gene (L2G) scores are an attempt at overcoming the challenges of establishing causal relationships between variants and genes. The authors employed a machine learning-model to integrate fine-mapping with functional genomics data and *in silico* predictions to link GWAS loci to their target genes (Mountjoy et al., 2021). The output L2G scores are calibrated to represent the probability (0, 1) that the

Regulatory Build

The Ensembl regulatory build compiles a summary of putative regulatory regions found in the human genome. It is built on the basis of publically available epigenetic marks and transcription factor binding and contains Promoters, Proximal enhancers, distal enhancers and CTCF binding sites (Zerbino et al., 2015).

ENCODE cCREs

Very similarly the ENCODE project summarizes DNA accessibility and chromatin modification data into candidate cis-regulatory elements. Regions showing high DNase signal are further annotated to be proximal enhancer-like elements (pELS) or distal enhancer-like elements (dELS), promoter-like elements (PLS), other high-H3K4me3 (which might represent poised or non-canonical promoters), or CTCF-only elements based on the existence of H3K4me3, H3K27ac and CTCF signals. (*SCREEN: Search Candidate Regulatory Elements by ENCODE* n.d.; Moore et al., 2020)

scATAC Seq

ATAC-seq is a method to access chromatin accessibility in the genome. ATAC seq utilizes the hyperactive Tn5 transposase to insert sequencing adapters into accessible regions of chromosome. DNA is purified and amplified via PCR and can be sequenced. Mapping these insertions to the genome allows for the identification of highly accessible genomic regions (Buenrostro et al., 2013; Buenrostro et al., 2015a).

PCR amplification of the DNA makes this method extremely sensitive. Pushing the requirement of biomaterial to the minimum, ATAC seq is applicable on a single cell level. For scATC seq, a individual cells are isolated and the their DNA tagged with barcoded primers during the PCR. These barcodes allow mapping of ATAC-seq single to the isolated celltype in data processing (Buenrostro et al., 2015b).

ABC Model

(Fulco et al., 2019; Nasser et al., 2021) The ABC model grants isghts into potential cell specific enhancer-gene interactions based on chromatin state, outperforming previuosly used methods.

$$ABC\ score_{E,G} = \frac{A_E \times C_{E,G}}{\sum_{all\ elements\ e\ within\ 5\ Mb\ of\ G} A_e \times C_{e,G}}$$

Generally speaking model incorporates the activity of an enhancer A_E as well as con-
tacts with the gene of interest $C_{E,G}$, normalized by the total effect of all elements in the
area.

Hi-C & TADs

Hi-C is a methods for mapping chromosomal conformation. For achieve this, genome asso-
ciated proteins are cross-linked with formaldhyd, DNA is digested with restriction enzymes
and generated overhangs are filled in with biotinylated nucleotides. The resulting fragments
are ligated to covalently link DNA fragments which were originally in close spatial proxim-
ity. The DNA is purified and fragmented, allowing the pulldown of fragments containing
junctions sites via the filled in biotin tags. After sequencing of the enriched fragments, their
sequences and mapped to the genome, identifying interacting DNA regions (Lieberman-
Aiden et al., 2009; Wit and Laat, 2012).

Looking at Hi-C data, TADs were identified to be a basic featurer of genome orgnization
with an average size of 880 kb (Dixon et al., 2012; Wang et al., 2018b). What makes tads
of such high interest ist the circumstance, that interactions of DNA sequences are usually
confined within theses TADs. Tissue specific genes and thier enahncers are usually found in
the middle of TADs, while the edges enrich for housekeeping genes and CTCF binding sides
which migh serves as insulators betweent different domains (Pombo and Dillon, 2015).

1.7 Aim of the thesis

The aims of this thesis are split into two quite distinct projects:

1 Introduction

- The split role of PDGF-BB during progression of arteriosclerosis (see section [LINK TO SECTION]), indicates that PDGF-BB signaling is neither completely beneficial nor disadvantageous to the diseases but requires a sweet spot. Combined with the observation that ROS are a secondary messenger in PDGF signaling, we wish to evaluate the hypothesis, that the excessive PDGF signaling can cause oxidative stress. s

Further there is already a review on ROS in arteriosclerosis which I should read (Burtenshaw et al., [2019](#)).

- Further we would like to do some *in silico* stuff and build the GWAS Navigator.

Have fun with my thesis, this still is a mess...

2

Material

2.1 Manufacturers

Manufacturer	Seat
Agilent Technologies, Inc.	Santa Clara, CA, USA
Assistent - look this up	?! , DE
BRAND GMBH & Co. KG	Wertheim, DE
ChemoMetec A/S	Allerød, DK
Eppendorf AG	Hamburg, DE
Heraeus Holding GmbH	Hanau, DE
Merck KGaA	Darmstadt, DE
Keyence Corporation	Osaka, JP
Kisker Biotech GmbH & Co. KG	?! , DE
Sarstedt AG & Co.	Nürnberg, DE
Sigma-Aldrich Co. LLC.	St. Louis, MO, USA
Thermo Fisher Scientific Inc.	Waltham, MA, USA
Pepro Tech -> look this up	?!
Pechiney Plastic Packaging, Inc.	Chicago, IL, USA
J.T. Baker -> look up	?!
GFL mbH	Burgwedel, DE
AB -> look this up	Warrington, UK
Gibco BRL	Gaithersburg, MD, USA
(Brand of Thermo Fisher Scientific Inc.	
Ibidi -> look this up	

Continued on next page

(Continued)

Manufacturer	Seat
Invitrogen™ (Marke von Thermo Fisher Scientific Inc.) (Brand of Thermo Fisher Scientific Inc.)	
Lonza Group AG	Basel, CHE
Biosell -> look this up	
New England Biolabs GmbH	Ipswich, MA, USA
Nikon Corporation	Minato, JP
Sartorius ?!	Göttingen, DE
SensoQuest GmbH	Göttingen, DE
HANNA Instruments	??
Heidolph Instruments Labortechnik	Schwabach, DE
Ziegra Eis Maschinen	?! , DE

2.2 Antibodies

Name	Species	Manufacturer
8oxoG	?	?
other oxStress	?	?
Fibronectin	?	?
secondary ones	?	?

2.3 Celllines

Name	Celltype	Manufacturer
Human Aortic Smooth Muscle Cell (HAoSMC)	prim. human cell	

2.4 Primer

Target	Name	Sequence
CNN1	Fw	5'-seq-3'
	Rv	5'-seq-3'

Continued on next page

(Continued)

Target	Name	Sequence
GAPDH	Fw	5'-seq-3'
	Rv	5'-seq-3'
MMP9	Fw	5'-seq-3'
	Rv	5'-seq-3'

2.5 Chemicals

Name	Manufacturer
5X First Strand Buffer	Invitrogen™ (Marke von Thermo Fisher Scientific Inc.)
Antimycin A	Sigma-Aldrich Co. LLC.
BSA	?!?
CellROX	Thermo Fisher Scientific Inc.
Collagen Type I, rat tail	Ibidi -> look this up
dNTP Mix	AB -> look this up
DTT	Invitrogen™ (Marke von Thermo Fisher Scientific Inc.)
Ethanol (concentration?)	J.T. Baker -> look up
FCCP	Sigma-Aldrich Co. LLC.
D-Glucose	Sigma-Aldrich Co. LLC.
GlutaMAX™-I	Gibco BRL
Hoechst	?!?
IL-1	Pepro Tech -> look this up
M-MLV RT	Thermo Fisher Scientific Inc.
NAC	Sigma-Aldrich Co. LLC.
NaHCO ₃	Carl Roth GmbH + Co. KG
NaOH, 1 N	Carl Roth GmbH + Co. KG
Oligomycin	Sigma-Aldrich Co. LLC.
Roth Hexanukleotid Random-Primer	Carl Roth GmbH + Co. KG
PBS	Lonza Group AG
PDGF-BB	Pepro Tech -> look this up
Sodium Pyruvate	Gibco BRL
RiboLock R	Thermo Fisher Scientific Inc.

Continued on next page

(Continued)

Name	Manufacturer
Seahorse XF calibrant	Agilent Technologies, Inc.
PowerUp TM SYBR TM GREEN Master Mix	Thermo Fisher Scientific Inc.
TGF β	Pepro Tech -> look this up

2.6 Media, Supplements

Name	Manufacturer
FBS Gold Plus	Biosell -> look this up
Medium 231 (M231)	Gibco BRL
Smooth Muscle Cell Growth Supplement	?!?
XF Base Medium	Agilent Technologies, Inc.

2.7 Solutions

Name	Manufacturer
Interleukin 1 beta (IL-1)	IL-1 0.1 % BSA in PBS
N-Acetylcystein (NAC)	0.25 M NAC in water, ~pH 7
Platelet-derived growth factor-BB (PDGF-BB)	PDGF-BB 0.1 % BSA in PBS
Transforming Growth Factor beta (TGF)	TGF β 0.1 % BSA in PBS

2.8 Kits

Kit	Manufacturer
Total RNA Purification Kit	Jena Bioscience GmbH

2.9 Consumables

Name	Manufacturer
Quali-PCR-Tubes 0,2 mL	Kisker Biotech GmbH & Co. KG
Quali-PCR-Tubes 0,5 mL	Kisker Biotech GmbH & Co. KG
SafeSeal Gefäß 1,5 mL	Sarstedt AG & Co.
SafeSeal Gefäß 1,5 mL	Sarstedt AG & Co.
SafeSeal Gefäß 5 mL	Sarstedt AG & Co.
NUNC MULTIDISH 24	Thermo Fisher Scientific Inc.
Agilent Seahorse XF24 Cell Culture Microplate	Agilent Technologies, Inc.
Agilent Seahorse XF24 Extracellular Flux Assy Kit	Agilent Technologies, Inc.
384 Well Multiply PCR plates	
Pasteurpipetten ISO 7712	Assistent - look this up
Pipette tip 20 µL	Sarstedt AG & Co.
Pipette tip 200 µL	Sarstedt AG & Co.
Pipette tip 1000 µL	Sarstedt AG & Co.
Filter tip 20 µL	Sarstedt AG & Co.
Filter tip 200 µL	Sarstedt AG & Co.
Filter tip 1000 µL	Sarstedt AG & Co.
BD Discardit™II	?!?
0,20 µm filter	?!?
Via1-Casette™	ChemoMetec A/S
Tube 15 ml	Sarstedt AG & Co.
Tube 50 ml	Sarstedt AG & Co.
Serological pipette 5 mL	Sarstedt AG & Co.
Serological pipette 10 mL	Sarstedt AG & Co.
Serological pipette 25 mL	Sarstedt AG & Co.
Serological pipette 50 mL	Sarstedt AG & Co.
Parafilm®M	Pechiney Plastic Packaging, Inc.
TC Flask T75, Cell+, Vented Cap	Sarstedt AG & Co.
CRYSTAL qPCR-Folie	New England Biolabs GmbH

2.10 Devices

Name	Manufacturer
Bench Heraus	Heraeus Holding GmbH
Bench 2	
Research pipettes (2.5µL, 10 µL, 100 µL, 1000µL)	Eppendorf AG
Hera Cell	Heraeus Holding GmbH
Hera Cell 150	Heraeus Holding GmbH
NucleoCounter NC-200	ChemoMetec A/S
Incubation/Inactivation bath 1083	GFL mbH
Centrifuge 5702 R	Eppendorf AG
Eclipse TS100	Nikon Corporation
pipet X rainin	!/?
Centrifuge 5415 R	Eppendorf AG
Rotana 460 R	Andreas Hettich GmbH & Co. KG
XF24 Extracellular Flux Analyzer	Agilent Technologies, Inc.
7900HT Fast Real-Time PCR System	Thermo Fisher Scientific Inc.
LA 120 S	Sartorius ?!
Reax Top	Heidolph Instruments Labortechnik
MR 3001	Heidolph Instruments Labortechnik
BZ-X810 All-in-One Fluorescence Microscope	Keyence Corporation
BZ-X800 All-in-One Fluorescence Microscope POWER	Keyence Corporation
SensoQuest labcycler	SensoQuest GmbH
pH 221 Microprocessor pH Meter	HANNA Instruments
NanoDrop 2000	Thermo Fisher Scientific Inc.
Ice machine	Ziegra Eis Maschinen

2.11 Programs & Modules

Programs

Program	Version	Manufacturer
Affinity Designer	1.10	Serif (Europe) Ltd.
Excel	Version 2205	Microsoft Corporation
GitHub		GitHub, Inc

Continued on next page

(Continued)

Program	Version	Manufacturer
keyence software?!		
MiKTeX	2.9	Christian Schenk
python	3.9	Python Software Foundation
PyCharm (Community edition)	2021.2.2	JetBrains s.r.o.
SchemaSpy	5.0.0	John Currier
SDS	2.2.2	Thermo Fisher Scientific GmbH Im
sqlite3_analyzer	3.38.5.	The SQLite Consortium
Wave Controller	2.6.3	Agilent Technologies

Python Modules

Module	Version	Info
beautifulsoup4	4.11.1	crummy.com/software/BeautifulSoup
bokeh	2.4.1	bokeh.org
numpy	1.21.4	numpy.org
pandas	1.3.4	pandas.pydata.org
Pillow	8.4.0	python-pillow.org
pylifter	0.4	github.com/konstantint/pylifter
python standard library	3.9	docs.python.org
matplotlib	3.4.3	matplotlib.org
requests	2.26.0	requests.readthedocs.io
scipy	1.7.3	scipy.org
seaborn	0.11.2	seaborn.pydata.org
urllib3	1.26.7	urllib3.readthedocs.io
wget	3.2	bitbucket.org/licface/pywget

Frameworks

- This thesis was generated with the [uzl-thesis class](#) have been written and kindly provided by Till Tantau.
- Styling of the GWAS Visualizer was done with the [CSS Framework Bootstrap](#).

2.12 Public Data

3

Methods

3.1 Cultivation and differentiation of HAoSMCs

For the following experiments human aortic smooth muscle cells (HAoSMCs) were used. A cell type commonly used for the study of cardiovascular function and disease [Reference for this claim]. Cells were kept at 37°C and 5% CO₂ when ever possible.

Cells were differentiated treated first with TGF β and then with Interleukin 1 beta (IL-1) & PDGF-BB to induce a synthetic phenotype. For more information please check the section [1.2](#) on smooth muscle cells in CAD.

Thawing & Cultivation

Cells were cultivated to a maximum passage of 10, after that new passage cells were thawed. For long time storage cells were kept in [cryo medium] and stored in liquid nitrogen. When required, new cells (6th passage) were need cells were thawed at 37°C in the water bath and transfered to a falcon. After centrifugation for 2 min at 300xg the supernatant was removed and the cell pellet taken up in 14 mL of M231 + Smooth Muscle Cell Growth Supplement (SMGS) for cultivation in a T75 flask. Every other day 2/3 of the medium were removed and replaced by fresh.

Passaging

When reaching a maximum of 80% confluency (approx. once a week) the medium was removed completely and cells were washed once with 5 mL of phosphate buffered solution (PBS). Then the cells were incubation with 3 mL trypsin for 4 min at 37°C. After 7 mL M231 were added to the deattached cells and the cells were transfered to a falcon and pelleted for 4 min at 300xg. The supernatant was removed and the pellet resuspended in M231 + SMGS, seeding 500×10^3 cells per T75 flask.

Preparation of Collagen I matrix

For preparation of the collagen type I (col I) matrix (1.8 mg/mL) all the components were mixed, adding the collagen last. All components were stored at 4°C and all pipetting steps were carried out on ice:

Table 3.1: col I Matrix Composition

component	concentration	volume (μL)
H2O	-	38.9
M231	-	53.3
SMGS	20x	5,3
NaOH	1 M	2,7
NaHCO ₃	7.5 %	2.1
Col I	5 mg/mL	57.6
total	-	160

160 μL of matrix mix were transferred in each used well of a 24-well plate, fully coating the bottom of the well. For polymerization the matrix was incubated at 37°C for at least 60 min.

Differentiation of HAoSMCs

Differentiation was carried out in 24 wells plates with 1 mL M231 supplemented with 1 % fetal bovine serum (FBS) and different cytokines:

- **Day 0:** Matrix and cells were prepared as described in the sections Preparation of col I matrix and Passaging. Seeding of 40×10^3 in M231 + SMGS on plastic or on 160 μL col I matrix.
- **Day 1:** After 24 h the medium was replaced with 1 mL M231 + 1% FBS + 5 ng/mL TGF β (or just 1 mL M231 + 1% FBS).
- **Day 5:** The medium was replaced with 1 mL M231 + 1% FBS + 10 ng/mL IL-1 + 10 ng/mL PDGF-BB (or just 1 mL M231 + 1% FBS).
- **Day 7:** Potentially further stimulation described in the section of the used assay.

3.2 mRNA Quantification

quantative polymerase chain reaction (qPCR) was utilized to assess the mrribonucleic acid (RNA) concentration of the two reporter genes Calponin 1 (CNN1) and Matrix metalloproteinase 9 (MMP9) in HAoSMCs differentiated as described in section on differentiation. Using the house keeping gene Glyceraldehyde-3-phosphate dehydrogenase (GAPDH) for reference.

SYBR® Green is an intercalating deoxyribonucleic acid (DNA) dye that allows for the monitoring of DNA amplification. Flourescence is measured after every amplification cycle of the PCR yielding a crossing point when signal reaches a certain threshold. A lower quantification cycle (Cq) corresponds to an higher initial DNA concentration (Huggett and Bustin, 2011).

RNA Isolation

RNA was isolated using the kit and extraction was performed according to the corresponding protocol, using an extra washing step with 700 μL 80 % ethanol and eluting with 30 μL

of RNase-free water. Determination of nucleic acid concentration was carried out with the NanoDrop.

Reverse Transcription

For reverse transcription (RT), RNA samples were diluted to yield 10 μL of 10 ng/ μL RNA. The samples were heated for 5 min at 68°C before adding 10 μL of the RT reaction mix described in the following table:

Table 3.2: RT Master Mix

component	concentration	volume (μL)
First Strand Buffer	5x	4
DTT		2
dNTP		1
Oligos		1
RiboLock		1
M-MLVRT		1

The reaction was carried out for 60 min at 37°C before inactivating the enzyme for 5 min at 95°C. cDNA was used for qPCR or stored at -20°C.

qPCR

The samples were prepared in a 384-well plate using SYBR® Green Master Mix:

Table 3.3: qPCR samplesThe samples for the qPCR

component	concentration	volume (μL)
SYBR GREEN Master Mix	1:2	3.75
Primer (forward + reverse)	5 pM (each)	1.125
H ₂ O	-	1.125
cDNA	-	1.5

Wells were sealed, thoroughly mixed by inversion of the plate and the assay performed using following programme on the TaqMan:

Table 3.4: qPCR programmeThe programme for the qPCR

step	time (s)	temperature (°C)	loop to	passes
1	120	50		1
2	600	95		1
3	15	60		40
4	60	60	3	40
5	600	95		1
6	-	16		1

Processing of Data

The Cq was automatically calculated by the software SDS2.2.2 and exported for further analysis. The arithmetic mean of three 3 technical was calculated for each sample, disregarding values that are obvious outliers. For normalization the mean ct of the reference gene GAPDH was subtracted from the mean ct of the gene of interest:

$$\Delta ct = ct(\text{gene of interest}) - ct(\text{GAPDH})$$

Taking into account the exponential amplification of DNA in PCR, the Δct can then be transformed into an relative expression level. Where 10×10^6 is just a constant to yield values that are easier to work with:

$$\text{rel.expr.} = 2^{-\Delta ct \times 10^6}$$

In total four biological replicates were done. Data visualization and statistical analysis was done in python using the modules: pandas, numpy, scipy as well as pyplot and seaborn. Assuming a normal distribution, student's t-test was used, a p-value of 0.05 is considered as significant. For detailed information please check the script.

3.3 Energy Profiling

Seahorse Assay was utilized to assess the energy profile of HAoSMC differentiated as described in section on differentiation. For this assay cells were not differentiated in a 24 well plate but the seahorse plate, using 5 technical repeats and on control well for 4 tested conditions. Since the plate would not fit the matrix cells were cultivated in plastic!

The Seahorse XF Analyzer allows real time measurement of dissolved oxygen and protons in a confined small volume by using solid state sensor probes. These are used to calculate the oxygen consumption rate (OCR) and extracellular acidification rate (ECAR) of a cell monolayer. The OCR and ECAR are indicators for mitochondrial respiration and glycolysis respectively and can be used to assess the metabolic function of cells (**HowAgilentSeahorse**).

Seahorse Assay

On the day before the assay the Seahorse XF Analyzer was turned on to calibrate and the sensor cartridge was left to equilibrate in Seahorse XF calibrant over night at 37 °C (in non-CO2 environment).

On the day of the assay, cells were washed with 500 μ L PBS each and afterwards 500 μ L supplemented XF BASE medium were added, cells were left to incubate for 1 h at 37°C in non-CO2 environment. During this time toxins for disruption of the respiratory chain were prepared and added to the cartridge:

Table 3.5: toxins for seahorsetoxins for seahorse. :)

component	concentration in cartridge(μ M)	volume in cartridge(μ L)	concentration in well (μ M)
Oligomycin	14	55	1.4
FCCP	10	60	2.0
Antimycin	50	65	5.0

The compound catridge was loaded into the XF Analyser for calibration, after successful calibration the hydration catridge was replaced with the cell plate. Measurement was carried out as following:

- Calibration of the probes.
- Equilibration
- 3 Repeats of:
 - Mixing (1 min)
 - Pause (2 min)
 - Detection of OCR and EACR (4 min)
- Pause (2 min)
- Injection of 55 μ L Oligomycin
- 3 Repeats of:
 - Mixing (1 min)
 - Pause (2 min)
 - Detection of OCR and EACR (4 min)
- Pause (2 min)
- Injection of 60 μ L FCCP
 - Mixing (1 min)
 - Pause (2 min)
 - Detection of OCR and EACR (4 min)
- Pause (2 min)
- Injection of 55 μ L Antimycin
- 3 Repeats of:
 - Mixing (1 min)
 - Pause (2 min)
 - Detection of OCR and EACR (4 min)

Finally the medium was removed and cells were stained for 15 min with Hoechst (concentration in PBS) and photographed in the keyence to determine cell count for normalization.

Processing of Data

Cells were quantified using (what exactly does Tobias script do) with a python script provided by my supervisor Dr. Tobias Reinberger, cell count and the signal of the control wells were used to normalize the OCR and EACR calculated by the XF Analyzer with the accompanying software.

In total three biological were recorded of which one was excluded because no changes in OCR and EACR could be detected and cells detached from the bottom of the wells during Hoechst staining. For the remaining two replicates the least fitting of the 5 technical repeats for each condition was manually excluded.

Further, again using a modified python script provided by Dr. Tobias Reinberger. Assuming a normal distribution, student's t-test was used, a p-value of 0.05 is considered as significant. For detailed information please check the script.

3.4 Oxidative Stress Assay

CellROX Green assay was used to assess generation of reactive oxygen species in HAoSMC differentiated as described in section on differentiation, after further stimulation (from here on referred to as 'boost') with PDGF. Additionally a recovery experiment was performed using NAC, a potent antioxidant, to quench generation of ROS. CellROX Green is a fluorescent dye that gets oxidized by ROS and then binds to DNA, showing bright green fluorescence (**CellROXGreenReagent**).

CellROX Assay

For the assay cells were washed with PBS then the boost was performed using variable concentrations of PDGF in 300 μ L HBSS. For ROS quenching with NAC, 0.25 M NAC solution was added to the wells 2 h prior to the experiment and also added to HBSS during the experiment.

Table 3.6: Seahorse Assay

component	concentration	final concentration	volume (μ L)
HBSS	-	-	300
PDGF	?	variable (0 - 400 ng/mL)	variable
Hoechst	?	?	0.3
CellROX (1:500)	?	?	0.6
NAC	0.25 M	variable (0 - 8 mM)	variable
total	-	-	~300

Cells further kept at 37°C in 5 % CO₂ environment, incubation time is indicated with the results of the respective experiment. Imaging was done at the keyence microscope using standard sensitivity and a exposure time of s in the green channel and s for the blue channel.

Processing of Data

For time resolved PDGF-BB boost titration 7 biological repeats were performed of which one was excluded because of high signal in the negative control. For NAC quench 4 biological repeats were performed of which one was excluded because no signal in the positive control. For quantification of signal intensity, pixels with a green value higher than 90 were counted. Differences in cell count were adjusted by division by the number of pixels with a blue value bigger than 80 (CHECK THRESHOLD VALUES!!). Z-STACK FOR THE NAC quench images. To adjust for large variance in total signal intensity between biological repeats, values were adjusted by division through the total signal of all recorded conditions. Mann Whitney U Test was used, a p-value of 0.05 is considered as significant. For detailed information please check the scripts.

3.5 Immunofluorescence

Fibronectin as marker of matrix. Used cells. Maybe also the anti-8-oxoG AB?

Protocol

First cells were washed with PBS and fixated for 40 min with 200 μ L -20°C methanol-aceton (1:1), after the removal of methanol-aceton cells were left to dry for 20 min. Then cells were treated for 30 min with 250 μ L permeabilization buffer, followed by 30 min with 250 μ L blocking buffer and incubated with 300 μ L of the primary AB over night at 4°C:

The next day the primary AB was removed and cells were incubated for 60 min at RT with the secondary AB:

After removal of the secondary AB cells were washed 3 times with PBS and stained for 15 min with DAPI (1:5000 in water).

Processing of Data

Me counting pixels.

3.6 Curation of Data for postGWAS Analyses

GWAS data and data for postGWAS analyses and co-visualization was downloaded from public resources. Processing of the data and further annotation is briefly described in the following listing. For a complete overview of all the data collected please refer to table or the download scripts. For explanation of the data please refer to the introduction or the sources themselves.

- **GWAS Summary Statistics:** The CAD GWAS summary statistics as well as a list of identified proxy SNPs from the study was annotated with [what did Tobias do] via the ensembl REST API by Dr. Tobias Reinberger.
- **HGNC Gene List** The newest quarterly update to the complete HGNC dataset was downloaded via the FTP server. The dataset was used to generate a list of all approved symbols, mapping to their HGNC id. Further a list of all symbols (approved, alias and previous) was generated, mapping to their HGNC id.
- **Linked SNPs** LD r^2 values for variants in a 500 kb window around all variants in the list of CAD GWAS proxy variants, were computed and downloaded via the ensembl REST API. For humans ensembl calculates the LD with data from the 1000 Genomes project (see table). In the same process linked SNPs were annotated with their most severe consequence (by VEP) via the ensembl REST API.

Table 3.7: 1000 Genomes Populations

Name	Size (individuals)	Description
1000GENOMES:phase3:ALL	2504	All phase 3 individuals
1000GENOMES:phase3:AMR	347	Americans
1000GENOMES:phase3:EAS	504	East Asians
1000GENOMES:phase3:EUR	503	European
1000GENOMES:phase3:SAS	489	South Asian

- **Ensembl Genome Annotation** The newest ensembl build (ensembl release 106) was downloaded via the FTP server. Features annotated as genes of the type protein

coding, lncRNA or miRNA were extracted, further gene symbols were mapped to their HGNC id if possible.

- **Open Target Genetics l2g Scores** The latest list of Open Target Genetics l2g Scores was downloaded via the FTP server. Entries were annotated with their HGNC ID when ever possible, entries that do not map to a gene that is approved by the HGNC were dropped.
- **Ensembl Regulatory Build** The newest ensembl regulatory build (ensembl release 106) was downloaded via the FTP server.
- **TSS** Transcription start sites for protein coding genes were extracted from a USCS Brower dump.
- **Associated traits from GWAS catalog** The SNP trait associations from the latest release of the GWAS catalog as well as the accompanying list of studies was downloaded via the FTP server. SNP-trait correlations missing a the position or a p-value for the association were dropped from the data set. Further the column for Odds Ratio or beta was separated in to two columns.
- **TADs** The data on TAD was downloaded via the download link on the 3D genome browser. Originally predicted by (Dixon et al., 2012).
- **scATAC-seq from Miller et al.** The processed scATAC seq data was scraped from the Miller Lab GitHub repository.
- **scATAC-seq from CATlas** The processed scATAC seq data was scraped from the Ren Lab website.
- **ABC model** The ABC model data was downloaded from the Engreitz Lab FTP server. The data was translated from Hg19 to Hg38 with pyliftover.
- **ENCODE cCREs** Done by Dr. Tobias Reinberger.

3.7 Visualization of GWAS data

For visualization of the data, an bokeh application was build, that fetches the data from the database and renders it to a webbrowser.

Bokeh is a python module that allow easy and interactive visualization of data. It combines the powerful data processing tools of python with the interactivity of JavaScript running in the browser. The python side of bokeh creates python objects which are serialized into JSON data and handed over to bokehJS which deserializes them into JavaScript objects that are rendered to the browser. The intergrated bokeh server additionally offers the possiblity to synchronize data between the underlying python environment and browser side JavaScript library, allowing real time updates to the displayed data.

According to good design principles the concerns of the application are split into two sections. Reading of data from the database and further processing steps are managed by a data provide and enclosed in one class. In contrast to the model-controler-view architecture, a popular architectural pattern for the design of user interfaces, there is no partition between a view and a controler. Since data visualization as well as the control widgets are created by bokeh, it is convenient to use the build in event listeners of the library to handle the required callbacks. Therefore the main file is responsilbe for the creation of all plots and widgets as well as listening for inputs.

STYLING USING A bootstrap thingy

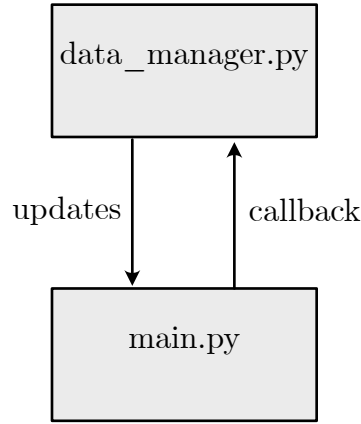


Figure 3.8: Architecture of the vis tool

3.8 Enrichment analysis

Based in the data in the database initial postGWAS studies were run. Annotation enrichment analyses are a popular tool for the identification of terms that are over-represent in a list of interest. The most prominent application probably being their application as gene set enrichment analyses (GESA). GESA are used to check for the over-representation of a candidate gene list in a predefined set of genes (Tipney and Hunter, 2010). In this case the method is used to determine if regulatory elements which overlap with SNPs associated with CAD are enriched in a biosample, using fisher’s exact test.

As a list of regulatory elements the cell type specific cCREs that are part of the ENCODE project were used (excluding cCREs marked as unclassified). As a list of SNPs the list of CAD associated proxy SNPs and linked variants (european population, $r^2 \geq 0.6$) was used. The four values required for calculation of the enrichment factor () and p-value require are shown in the Contingency of figure:

- Number of distinct cCREs among all biosamples (m)
- Number of distinct cCREs that are annotated in the biosample of interest (m_t)
- Number of distinct cCREs that overlap with a SNP in the SNP list in any biosample (n)
- Number of distinct cCREs that overlap with a SNP in the SNP list in the biosample of interest (n_t)

The p-value for the number of overlaps to be greater than or equal to the observation can be calculated as the cumulative distribution function of the hypergeometric distribution.

$$P(\sigma_t \geq n_t) = \sum_{k=n_t}^{\min(m_t, n)} \frac{\binom{n}{k} \binom{m-n}{m_t-k}}{\binom{m}{m_t}}$$

To account for the multiple comparisons problem, p-values were adjusted with Bonferoni correction where n is the number of tests (\equiv number of biosamples):

$$p_{adj.} = p * n$$

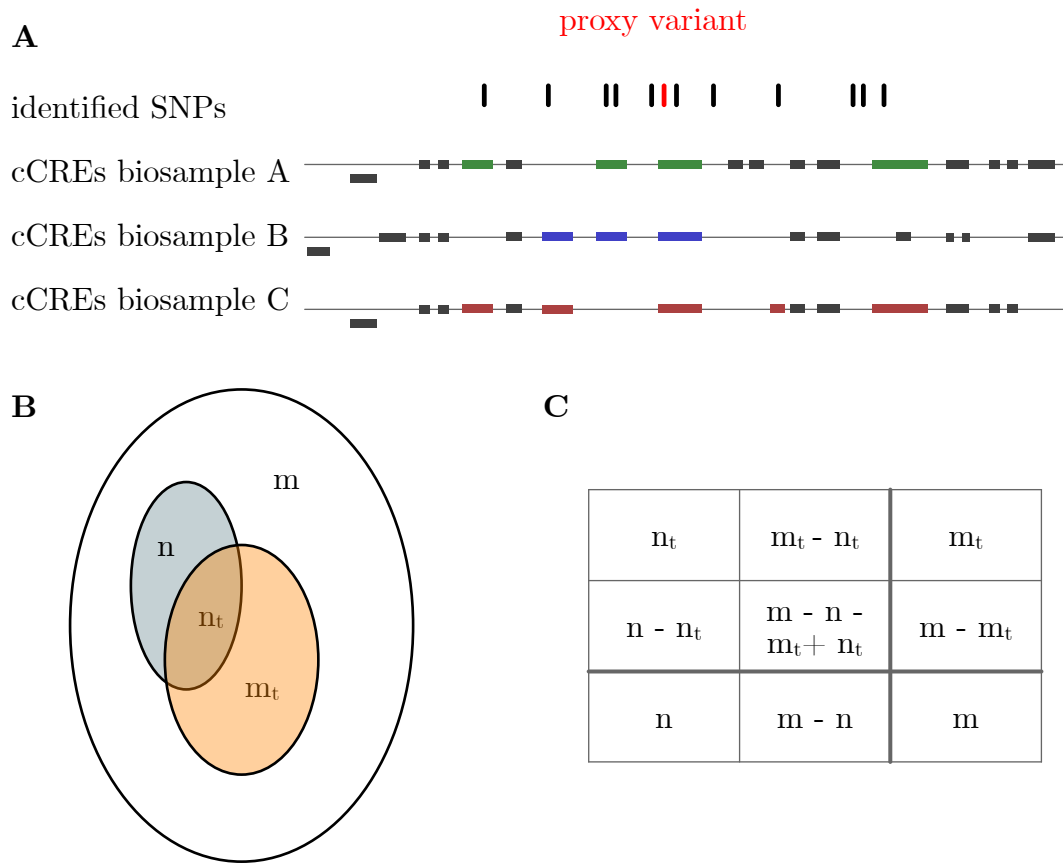


Figure 3.9: enrichment

The analysis and visualization were done in python. A p-value of 0.05 is considered as significant. For detailed information please check the analysis script and the visualization script.

4

Results

4.1 Differentiation

To generate a controllable phenotype, that is representative for the synthetic phenotype in vivo, HAoSMC were first treated for two days with $TGF\beta$ to induce a phenotype that resembles the contractile phenotype. Using this contractile phenotype as a precursor, cells were further treated for four days with IL-1 and PDGF-BB which should induce differentiation into the synthetic phenotype.

Expression of CNN1 & MMP9

To track the differentiation and confirm the protocol, the HAoSMCs were characterized using qPCR, assessing mRNA levels of CNN1 as a contractile marker and MMP9 as a synthetic marker. For better comparability mRNA levels are considered in relation to the house keeping gene GAPDH.

As seen in figure 4.1, stimulation of HAoSMCs cultivated on a col I-Matrix with $TGF\beta$ causes a significant increase in CNN1 expression, while not significant with four repeats, expression of CNN1 seems to drop off after further stimulation with IL-1 & PDGF-BB. The same trend, even if not as pronounced and not significant with four biological repeats, can be observed for HAoSMCs cultivated on plastic. Expression of MMP9 is not significantly different between any of the tested conditions, still a trend can be observed, that cells cultivated on the col I-matrix seem to show higher expression of MMP9.

Energy profile

Further the energy profiles of the cells were assessed via Seahorse Assay. oxygen consumption rate (OCR) and extracellular acidification rate (ECAR) for HAoSMCs differentiated under the same conditions as for qPCR are displayed in figure 4.2.

It is important to note, that the assay was carried out on plastic because the matrix does not fit into the confined compartment created by the piston for detection of OCR & ECAR. The OCR shows an expected drop after inhibition of the ATP synthase with Oligomycin, they further show a great increase after decoupling with Carbonyl cyanide-p-trifluoromethoxyphenylhydrazone (FCCP) and a steep drop-off after inhibition of coenzyme Q-cytochrome c reductase (complex III) with Antimycin A. Characteristics of the respira-

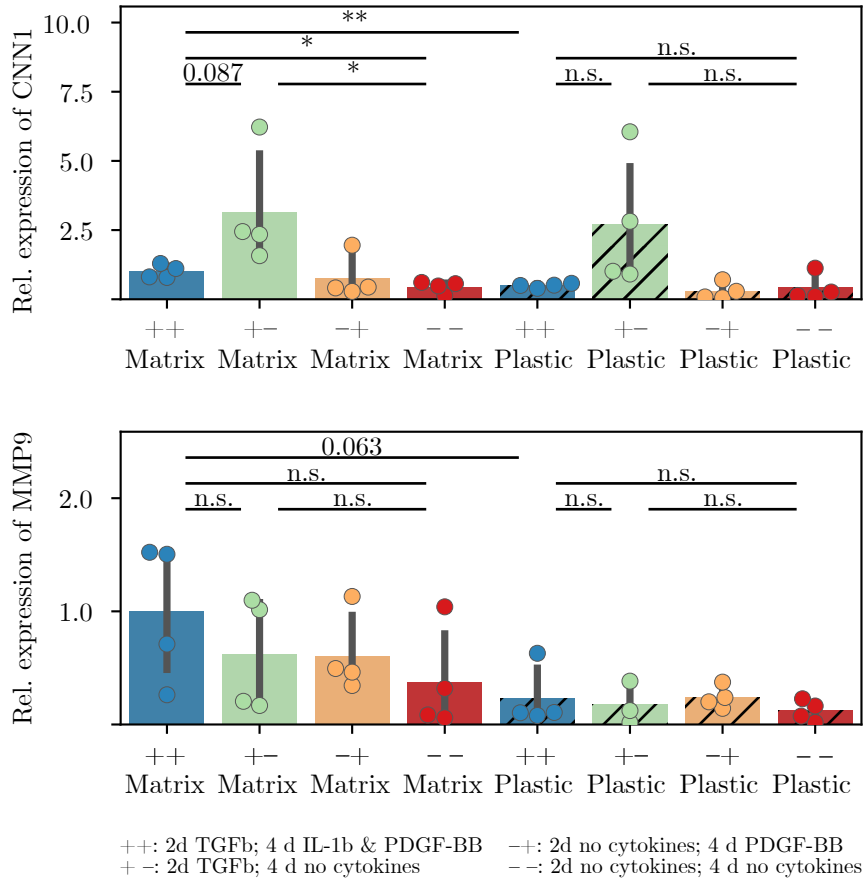


Figure 4.1: Relative Expression of CNN1 & MMP9 in HAoSMCs

qPCR analysis of expression for contractile marker CNN1 (top) and synthetic marker MMP9 (bottom) for HAoSMCs differentiated with different combinations of cytokines: ++: 2 d with TGF β followed by 4 d with IL-1 & PDGF-BB; +-: 2 d with TGF β followed by 4 d without stimulation; -+: 2 d without stimulation followed by 4 d with IL-1 & PDGF-BB; --: 6 d without stimulation. All four conditions were tested on two different surfaces (plastic vs. collagen 1 matrix). Expression levels are in relation to expression of housekeeping gene GAPDH. Statistical analysis for (n = 4) biological repeats was performed using student's T-test: * : $p < 0.05$; ** : $p < 0.01$

tory chain were calculated as described in section 3.3. Looking at the energy profile of the cells it is easy to see that OCR & ECAR are quite similar for the conditions ++, +- and --. The only outlier showing a higher ECAR, are HAoSMCs only stimulated with IL-1 & PDGF-BB (fig. 4.3, A).

More interesting difference can be observed when examining characteristics of the respiratory chain. Stimulation with only TGF β causes a significant decrease in basal respiration, ATP production, maximal respiration as well as spare capacity (figure 4.3, B top). Further stimulation with IL-1 & PDGF-BB then causes again significant increase of these parameters to similar levels as in undifferentiated HAoSMCs. Finally, it needs to be considered that

these observations are only based on two biological repeats done in plastic! To draw solid conclusions from seahorse assay, more biological repeats would be required.

4.2 Evaluation of oxidative Stress

It was evaluated if further stimulation of the induced synthetic phenotype with higher concentrations of PDGF-BB would yield ROS generation to an extend that can't be compensated by the ROS defense.

PDGF boost of out cells induces oxidative stress

For this one repeats of an experiment already previously done in the group was carried out. Stimulating the four tested conditions for two hours with 200 ng/mL PDGF-BB in HBSS.

As displayed in figure 4.4 only stimulation for two days with TGF β , followed by 2 days with IL-1 & PDGF-BB, followed by 2 h boost with PDGF-BB was able to trigger noticeable generation of ROS.

Characterization of the CellROX Assay

To get a better understanding of the assay and its limits a titration was carried out. For this HAoSMCs differentiated into the synthetic phenotype were boosted with different concentrations of PDGF-BB and CellROX signal was detected after 60, 120, 180 & 240 minutes.

As is clear from figure 4.5, a large impact factor on signal intensity is PDGF-BB concentration during the boost. Over all biological repeats only negligible signal was visible for concentrations < 100 ng/mL, followed by a significant increase in signal at 200 ng/mL. Signal intensity for boost with 400 ng/mL was mixed, in some cases yielding even higher signal, in some cases collapsing. The second large influence that is clearly resolved in this assay is duration of the boost. After 120 min first signal is observable, intensifying at 180 min and 240 mins. At 240 min also medium signal can be observed for all the conditions, indicating an unspecific response.

While the trend within on biological repeat was consistent and reproducible, variance between repeats was almost to the same extent as differences between the conditions. Two potential causes that are out of control of the experimenter are degradation possible degradation of CellROX Green which should be used up within 6 month after delivery as well as the exact composition of the col I matrix since it was observed that intensity in the CellROX assay seems to correlate with col I concentration in the matrix (data not shown).

In an attempt at normalization (figure 4.6), trying for account for these external factors, all data points were selected that were used in all biological repeats and intensities were normalized by the cumulative intensity of all selected conditions. This is quite similar to normalizing to the highest signal observed for the biological repeat because signal at 200 ng/mL after 240 min has by far the biggest contribution to the cumulative value of the biological repeat.

Rescue of ROS production using NAC

Finally, trusting the trend over all trend of the titration, a rescue experiment was performed, to verify that observed signal in the CellROX assay was indeed due to generation of ROS.

For this ROS generation was quenched by the addition of 2, 4, or 8 mM of N-acetylcystein (NAC) Quenching the signal with NAC.

Confirmation that the signal is indeed due to generation of intracellular ROS.

Finally it should be noted, that the signal onyl build up over 15 - 20 minutes under the microscope after the cells were taken out of the incubator. This indicates that generateion of ROS might not exclusively triggered by PDGF-BB stimulation but also required additional contributors like the loss the optimized atmosphere of 37°C and 5 % CO₂ in the incubator. This might not have been noted during the titration assay, because cells were taken out of the incubator after one hour anyway to image all wells.

4.3 Database and GWAS Visualizer

This was quite a long process, tinkering around with different designs to get a working solution. For this use case visualization in the browser using a database as the backend was the final decision. Compare to fetching everything online -> slow and just grabbing everything from files -> extremely stressful to maintain.

Curation of Data

Describe what actually happend to the data, probably in the methods section. This should be pretty self explanatory. Just have a look at the table and figure.

Visualization

Building on the initially intended use case for the data a visualization tool was build as briefly described in the methods section, for more details please check the source code or just ask.

Describe what the tool can do. Search function for SNPs, also for genes, providing info for associated SNPs. Visualization of the window SNPs, including linked SNPs annotated with important info such as most severe consequence. Further the data is aligned with important stuff like overlapping genes (integrating l2g scores). Also enesembl regulatory build and TADs. Further a lot of cell specific data in the form of scATAC seq tracks and promotor gene links from the ABC model. These are also shown and for easier navigation grouped into different classes using cellosaurus. To have a better look a individual variants these can be clicked, only highlighting tracks that overlap with the specific selected variant.

For more information regarding the aligned data please check the correspig paragraph in the intrdocution.

4.4 Enrichment analysis

The only data that is not displayed in the plot are cCRE elements which were used for an enrichment analysis. Checking different biosamples for significant enrichment of candidate cis regulatory elementss (cCREs) that are overlapping with proxy SNPs identified in the CAD GWAS or variants that are in LD with these. The procedure is described described in methods.

4 Results

As seen in figure 4.9, statistical significant enrichment ($p_{adj.} < 0.05$) was observed for 34 biosamples. These biosamples were annotated using Cellosaurus data. The most prominent groups of associated tissues were heart (8), lung (7) and artery (6).

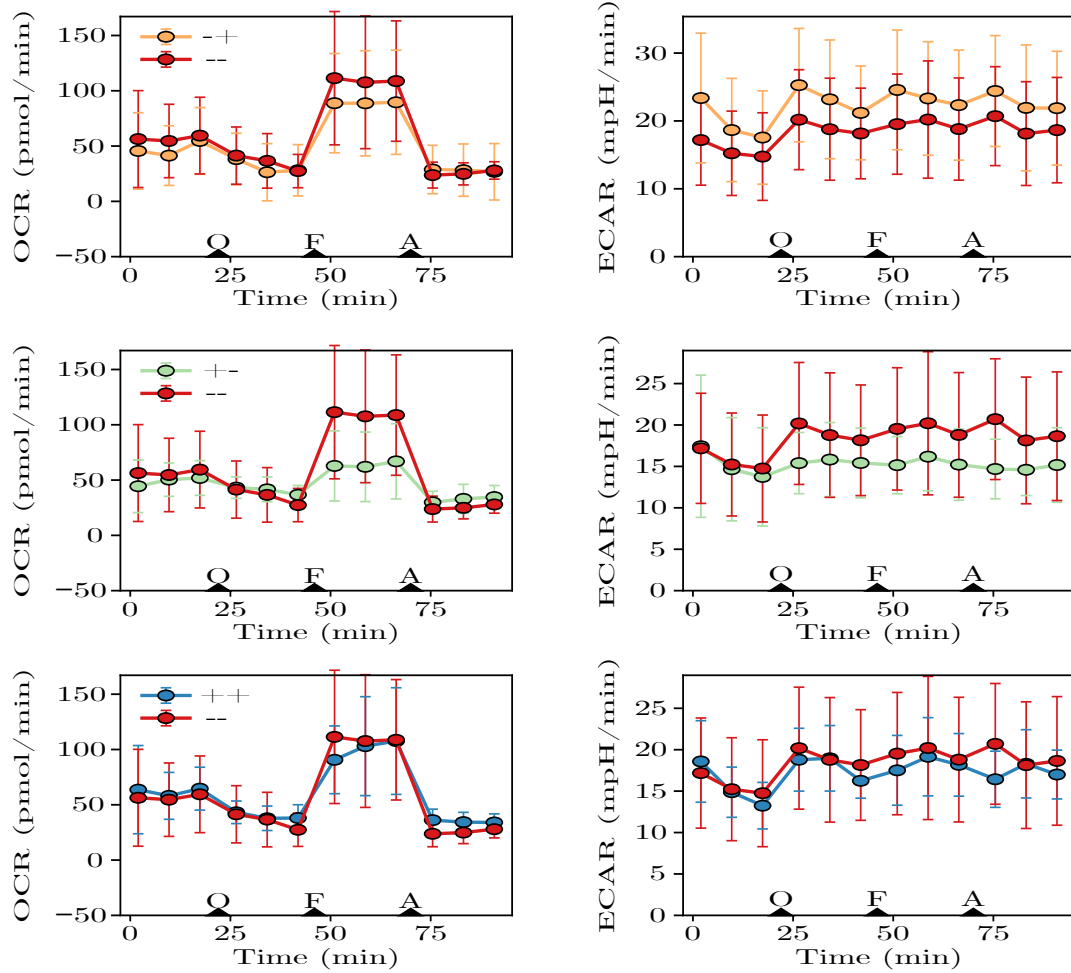


Figure 4.2: OCR & ECAR of HAoSMCs

Seahorse assay for HAoSMCs differentiated with different combinations of cytokines. ++: 2 d with TGF β followed by 4 d with IL-1 & PDGF-BB; +-: 2 d with TGF β followed by 4 d without stimulation; -+: 2 d without stimulation followed by 4 d with IL-1 & PDGF-BB; —: 6 d without stimulation. OCR & ECAR are shown for -+ (top), +- (middle) and ++ (bottom) in comparison to —. Injection times for toxins (O: Oligomycin; F: FCCP; A: Antimycin A) are marked as triangles. All tracks were recorded for cells cultivated on plastic. Shown datapoints are the average of (n = 2) biological repeats.

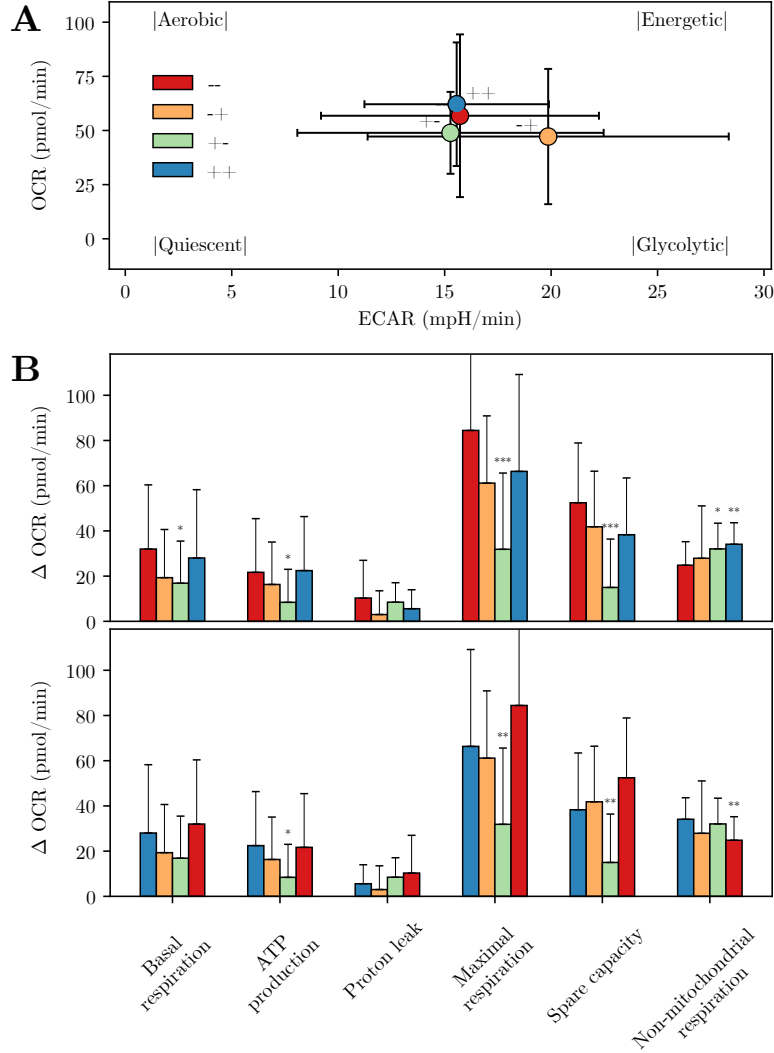


Figure 4.3: Energy profile of HAoSMCs

Seahorse assay for HAoSMCs differentiated with different combinations of cytokines. ++: 2 d with TGF β followed by 4 d with IL-1 & PDGF-BB; +-: 2 d with TGF β followed by 4 d without stimulation; -+: 2 d without stimulation followed by 4 d with IL-1 & PDGF-BB; -: 6 d without stimulation. (A) Initial OCR & ECAR of the four tested conditions. (B) Characteristics of the the respiratory chain calculated from the tracks shown in figure 4.2 as described in section ???. Statistical analysis for (n = 2) biological repeats was performed using student's T-test: * : $p < 0.05$; ** : $p < 0.01$; *** : $p < 0.001$

4 Results

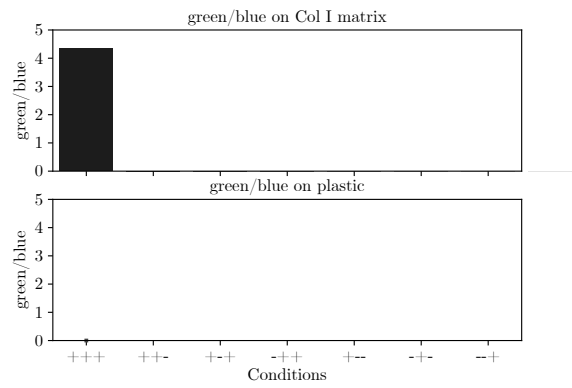


Figure 4.4: Stimulation with PDGF induces oxidative stress.
Repeat of the result already shown by Tobin.

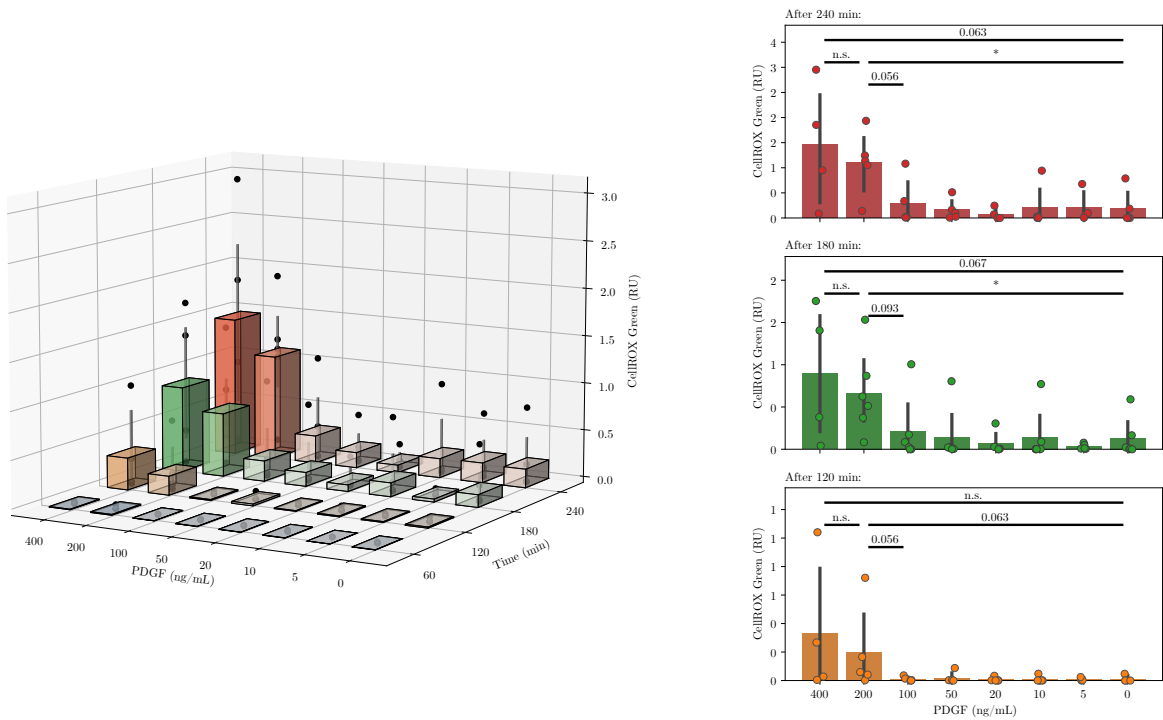


Figure 4.5: CellROX titration

4 Results

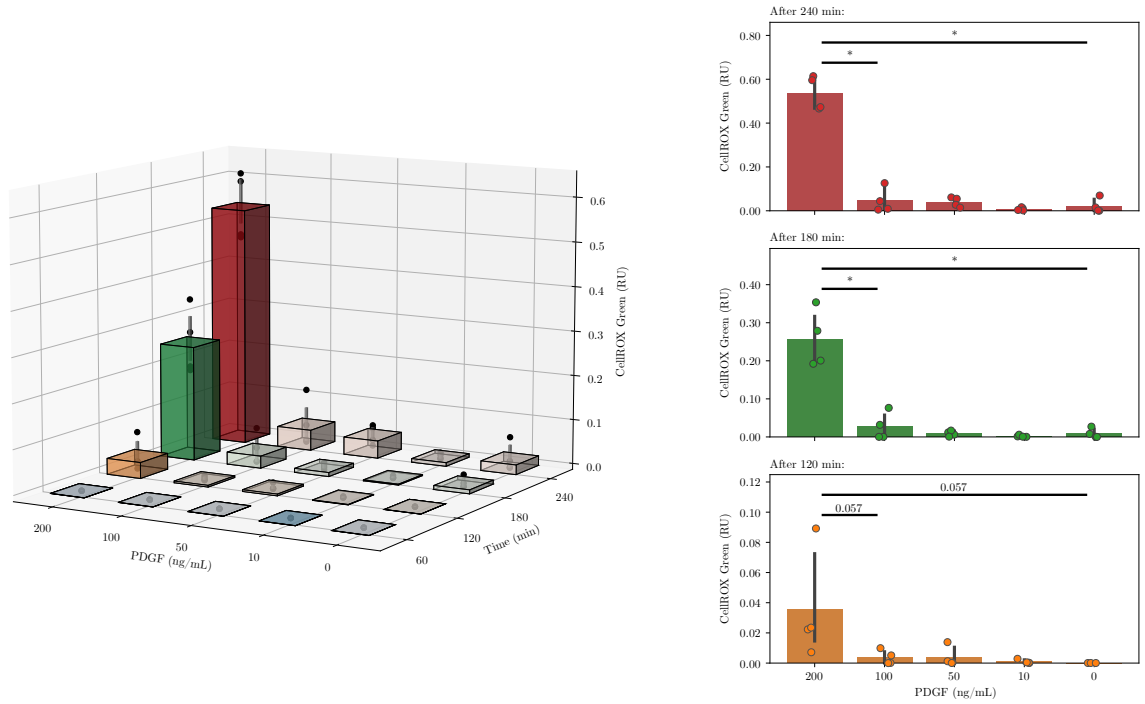


Figure 4.6: Stimulation with PDGF induces oxidative stress - normalized.

My attempt at normalization.

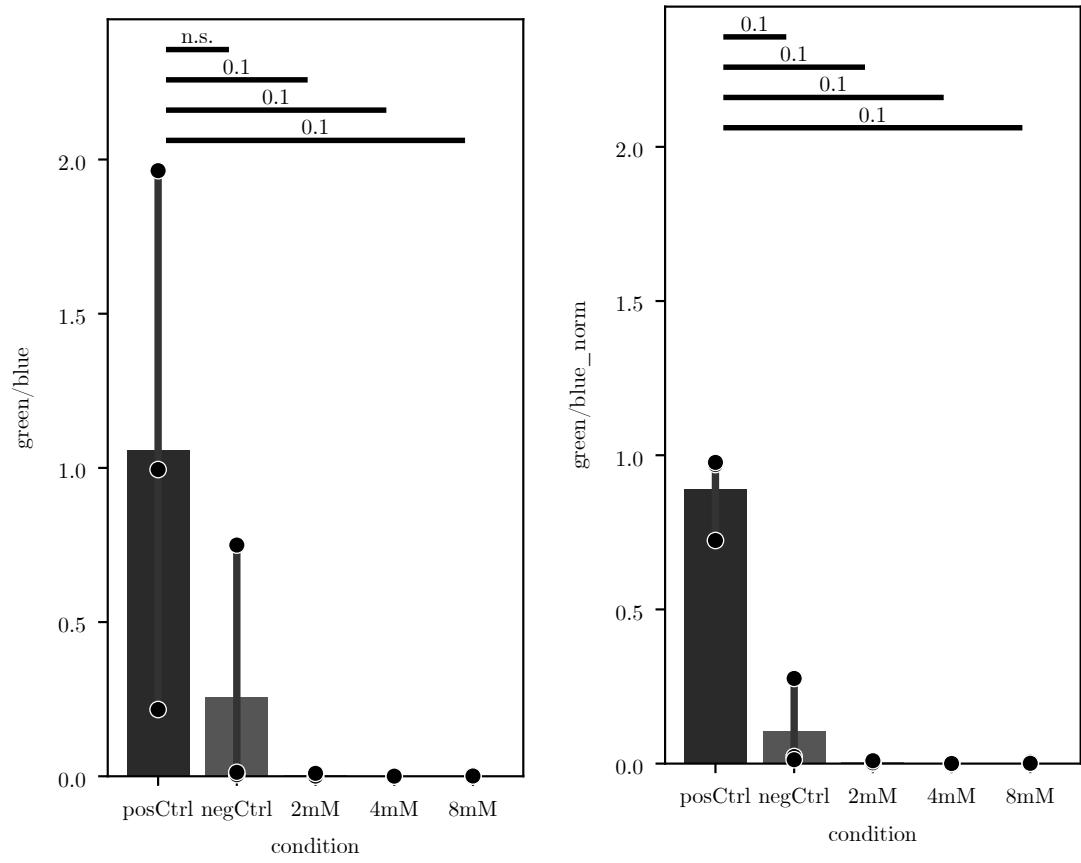


Figure 4.7: NAC quench

4 Results

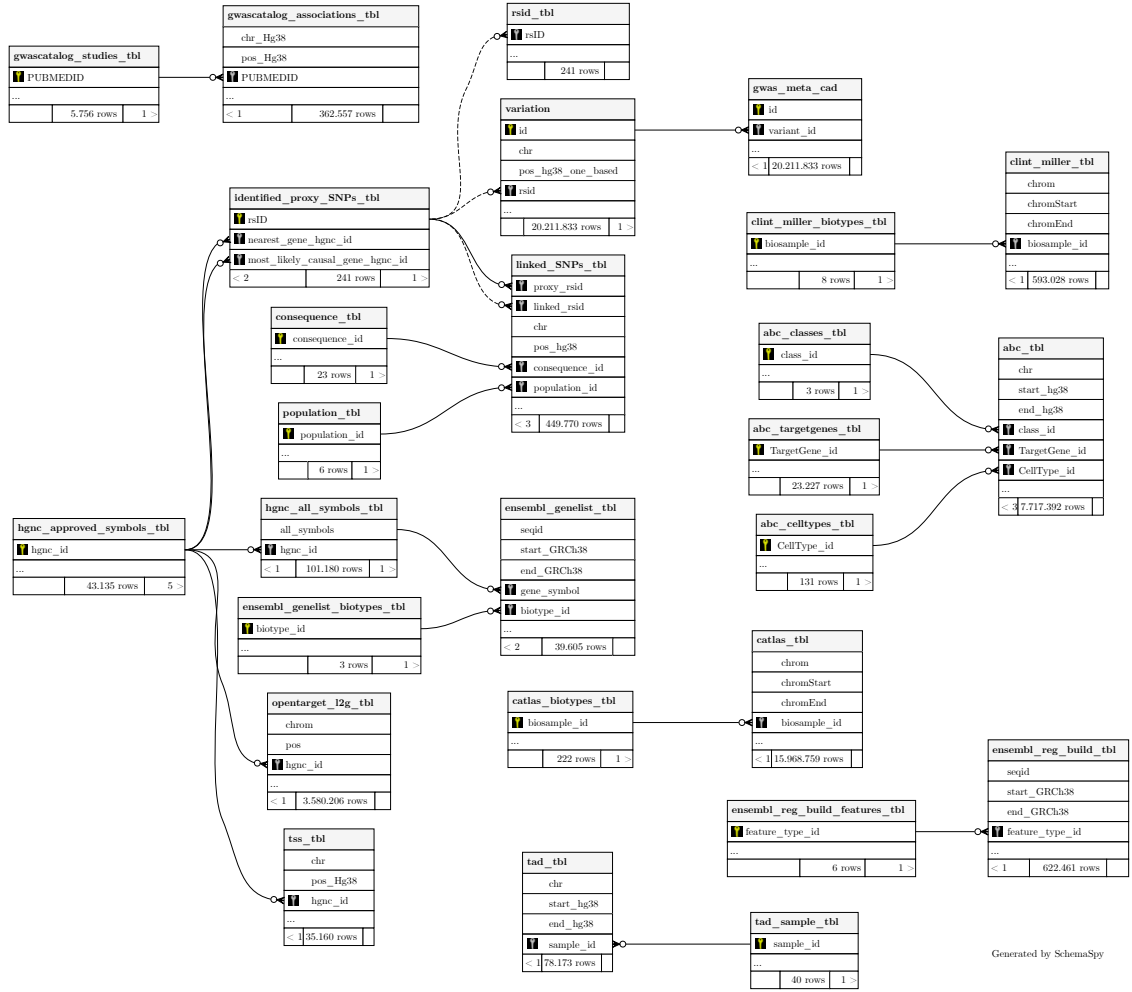


Figure 4.8: Entity-Relationship Diagram of the Database

4 Results

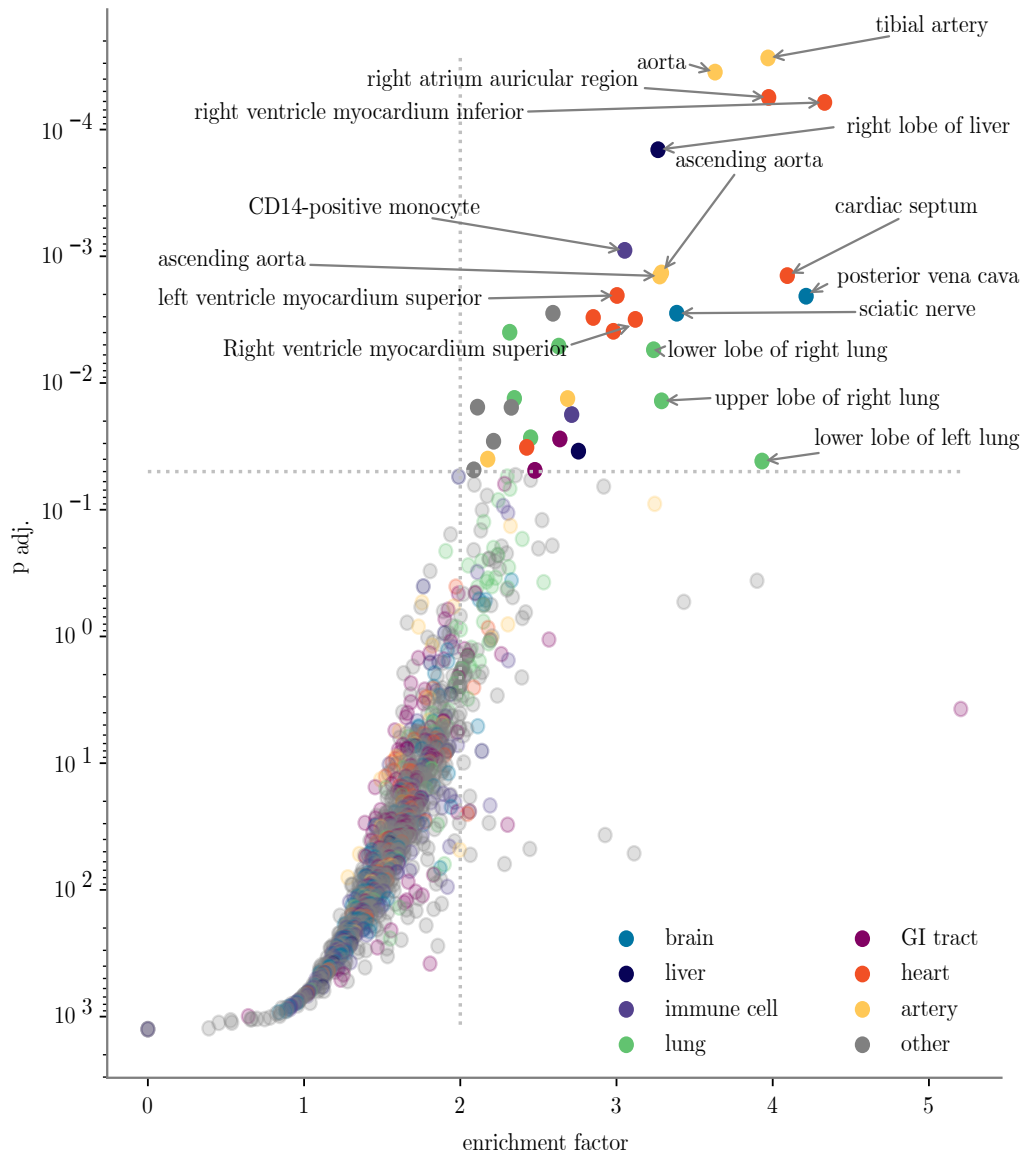


Figure 4.9: Enrichment Analysis This stuff actually seems to be working!!

Table 4.10: Enriched tissues

tissue	count in significant biosamples
heart	8
lung	7
artery	6
liver	2
GI tract	2
brain	2
immune cell	2
other	5
total	34

5

Discussion

Here I'll discuss my results should I ever finish the rest of my thesis.

SOME THING FOR ROS:

Recently, it was reported that STAT also has a cellular nongenomic function. STAT interacts with GRIM-19, a subunit of mitochondria respiratory complex I, which determines whether STAT3 is imported into mitochondria (12,13). Furthermore, there is direct evidence that STAT is present in the mitochondria of cultured cells and primary tissues. STAT mitochondrial importation selectively stabilizes and increases mitochondria respiratory complexes, allowing them to orchestrate responses to stimuli (14,15). As mitochondria respiratory complex I and III are thought to be the main source for ROS generation (16,17), it has been suggested that STAT1 facilitates ROS production and apoptosis (Lee et al., 2007). (Wang et al., 2018a)

Based on our results, STAT1, which is primarily induced by IFN- γ , is a potent effector responsible for ROS production and loss of $\Delta\Psi_m$ in LPS/D-GalN induced fulminant liver injury, evidenced by the finding that ROS production and loss of $\Delta\Psi_m$ were almost completely abrogated in STAT1(-/-) and IFN- γ (-/-) mice (Figure 2). \rightarrow INF induced ROS production and apoptosis.

SMC PHENOTYPES:

Contractile vs. synthetic VSMCs: loss of contractile marker and synthetic, migratory phenotype. Historically, this phenotypic switch was viewed as the hallmark of vascular repair. VSMCs retain their noncontractile status during atherosclerosis due to the continuous exposure to phenotypic switching-inducing stimuli

Foam cells: the majority of foam cells in atherosclerotic plaques appear derived from VSMCs. lipid loaded-VSMCs in culture secrete a variety of pro-inflammatory mediators⁴⁸ and undergo apoptosis from free cholesterol overload,⁴⁹ likely compromising plaque stability.

Macrophage-like: up-regulate 'macrophage markers', such as LGALS3, CD68,51 and pro-inflammatory cytokines. difficult to predict their impact on atherosclerotic plaque growth and stability. their pro-inflammatory profile, macrophage-like VSMCs are likely detrimental for plaque stability

Adipocyte-like: These studies emphasize again the high level of plasticity of VSMCs, but the role and abundance of adipocyte-like VSMCs in atherogenesis is unclear, illustrated by a postulated neutral-to-negative position on the 'plaque-stability scale'.

Osteochondrogenic: Vascular calcification is a tightly regulated process, primarily driven by VSMCs developing an osteochondrogenic phenotype. In particular, micro-calcified de-

posits (<50 mm) are associated with increased inflammation and mostly observed in the fibrous cap of human lesions, and thus considered detrimental for plaque stability. In contrast, macrocalcifications (>200 mm) often accumulate in the deep intima or necrotic core in organized structures and may promote plaque stability.

Myofibroblast-like: loss of Tcf21 inhibits phenotypic modulation and attenuates fibrocyte number in the fibrous cap, suggesting an athero-protective role (Figure 3).

EC-like: Direct evidence of endothelial-like VSMCs in human atherosclerosis is currently lacking.

MSC-like: The highly plastic nature of mesenchymal-like VSMCs offers the opportunity to therapeutically push these cells into a plaque-stabilising phenotype (Figure 3). The VSMCs undergo a ‘reprogramming process’ controlled by Kru  ppel-like factor 4 (KLF4) and can transdifferentiate into different cell types, including macrophage-like, EC-like, chondrocyte-like, and adipocyte-like under defined in vitro conditions.

Synthetic VSMCs play a major role in forming and maintaining the fibrous cap by secreting ECM, yet their overall role in plaque stability could be detrimental. Synthetic VSMCs secrete a wide variety of proinflammatory molecules and matrix-degrading enzymes that can cause cell death of neighbouring cells.^{42,114} Pro-inflammatory cytokines, such as IL1b, IL6, and MCP1 promote atherogenesis by stimulating monocyte recruitment and cell death¹¹⁹ and synthetic VSMCs express a range of adhesion molecules and receptors (e.g. Toll-like-receptors) that promote monocyte recruitment and regulate intracellular inflammatory signalling, respectively. Moreover, synthetic VSMCs secrete extracellular vesicles (EVs) that can drive vascular calcification (see Section 5.2.4).⁵⁹ Hence, synthetic VSMCs are beneficial for fibrous cap formation, but depending on the local environment and the disease stage, may promote inflammation, calcification, cell senescence, and plaque instability.

The contractile phenotype is positively controlled by the growth factor TGF  . PDGF-BB suppresses contractile gene expression via different mechanisms. (Grootaert and Bennett, 2021)

Vascular smooth muscle cells (VSMCs) play a key role in atherogenesis and have historically been considered beneficial for plaque stability.

Thinning of the fibrous cap in advanced plaques increases the risk of rupture, which triggers thrombus formation and subsequent clinical complications including heart attack and stroke (Libby et al., 2011; Tabas et al., 2015).

The model is rapidly evolving and adjusted: it isn’t even clear if cells migrate and proliferate or if they proliferate and migrate then.

The synthetic VSMC phenotype is characterised by loss of contractile marker expression and up-regulation of selective gene sets, including pro-inflammatory cytokines and MMPs, leading to increased cell migration, proliferation, and secretion of pro-inflammatory cytokines.

Therefore, it has been proposed that VSMC-derived cells can both improve plaque stability and exacerbate plaque rupture

To develop efficient therapeutic strategies to limit cardiovascular risk, additional knowledge about how specific VSMC-derived cell types function in mature plaque is therefore needed. Additionally, mechanistic insight into the regulation of VSMC plasticity is required to enable specific interventions. (Harman and J  rgensen, 2019)

Up until recently, vSMCs were classified as either contractile or dedifferentiated (ie,

synthetic).

The central dedifferentiated vSMC type that we classified is the mesenchymal-like phenotype.

The 3 main cellular layers forming the vessel wall are the adventitia, media, and the intima, surrounding the lumen. In the media, the middle layer, vascular smooth muscle cells (vSMCs) are the major cellular component. These vSMCs contribute to the integrity of the vessels and are able to adequately respond to stimuli of vasoconstriction and vasodilation.

For decades, vSMC activation and dedifferentiation has been regarded as the adoption of a single synthetic, proliferative phenotype. However, as revealed by recent scRNA-seq analyses, the diversity of vSMC phenotypes is far more sophisticated.

The combination of scRNA-seq and lineage tracing is extremely useful as it allows in-depth vSMC phenotypic characterization.

Contractile vSMCs are regarded as differentiated and quiescent cells under physiological conditions, expressing a panel of typical contractile proteins that is crucial to maintain vascular tension. Contractile vSMCs exhibit an elongated, spindle-shaped morphology and express a well-characterized set of contractile markers including smooth muscle actin (ACTA2), smooth muscle myosin heavy chain (MYH11), smooth muscle protein 22- α (SM22 /TAGLN), smoothelin (SMTN), and calponin (CNN1). Expression of these proteins is controlled by the transcription factors MYOCD (myocardin) and SRF (serum response factor), both of which are involved in the regulation of differentiation to contractile vSMCs.

In addition, external stimuli, such as TGF- β and heparin, play a pivotal role in promoting and maintaining the vSMCs contractile phenotype.

Once pathological processes in the vessel wall are initiated, vSMCs respond by changing their phenotype and function. A plethora of pathological cues induce these changes: factors from the circulation, compounds and proteins produced by activated endothelial cells, fibroblasts, perivascular adipocytes or inflammatory cells, (lack of) mechanical stress, damaged ECM protein fragments, or ECM-derived growth factors.

KLF4 is regulated by various signaling complexes at transcriptional and posttranslational levels.^{57,58} After exposure to PDGF-BB (platelet-derived growth factor BB), a stimulus of vSMC proliferation and phenotype switching, elevated levels of KLF4 were identified.

Induction of KLF4 in vSMCs results in a phenotypic switch from contractile to mesenchymal-like and initiates the expression of mesenchymal markers such as stem cell antigen-1 (SCA1)/LY6A, CD34, and CD44.^{40,41} During this transition, while gaining expression of mesenchymal markers, the contractile vSMCs lose expression of their contractile markers. (Yap et al., 2021)

To prevent or reverse the phenotypic transition to mesenchymal-like vSMCs, the expression of KLF4 can be suppressed by TGF- β or miR-143/145 to maintain the contractile vSMC phenotype.

Alternatively, mesenchymal-like vSMC may undergo further changes into other vSMC phenotypes.³¹

In addition, we argued that the data point in the direction of the mesenchymal-like cells giving rise to the other vSMC phenotypes; however, further experimental validation is needed to fully support this hypothesis. (Yap et al., 2021)

This includes the activation of SMC marker genes by TGF β 1 and contractile agonists such as angiotensin II as well as repression by PDGF BB.

inflammatory cytokines such as IL-1 can induce rapid downregulation of expression of multiple SMC differentiation marker genes (Alexander and Owens, 2012)

Using single-cell and bulk RNA-sequencing analyses of the brachiocephalic artery region and in vitro models, we provide evidence that SMC-to-MF transitions are induced by PDGF and transforming growth factor- and dependent on aerobic glycolysis, while EndoMT is induced by interleukin-1 and transforming growth factor-. Together, we provide evidence that the ACTA2+ fibrous cap originates from a tapestry of cell types, which transition to an MF-like state through distinct signalling pathways that are either dependent on or associated with extensive metabolic reprogramming.

xacerbated lesion development, suggesting that dysregulated EndoMT was detrimental for atherogenesis

SMC PDGFR signalling plays a critical role in SMC investment within the lesion and the fibrous cap. no significant differences in any of the indices of stability examined, including collagen content of the lesion and fibrous cap.

Indeed, sustained PDGFR signalling is essential for retention of ACTA2+ SMCs and collagen content within the fibrous cap, suggesting a critical protective role of PDGFR signalling in fibrous cap development and maintenance. Therefore, contrary to dogma, we propose that augmenting46 rather than reducing PDGFR signalling in SMCs during late-stage atherosclerosis would be a beneficial therapeutic strategy for maintaining lesion stability.

We have further shown that a PDGF/TGF- -induced shift in bioenergetic pathway directly affects ECM synthesis in cultured SMCs that have phenotypically modulated to a MF-like state.

Indeed, sustained PDGFR signalling is essential for retention of ACTA2+ SMCs and collagen content within the fibrous cap, suggesting a critical protective role of PDGFR signalling in fibrous cap development and maintenance. Therefore, contrary to dogma, we propose that augmenting46 rather than reducing PDGFR signalling in SMCs during late-stage atherosclerosis would be a beneficial therapeutic strategy for maintaining lesion stability.

SMC PDGFR signalling plays a critical role in SMC investment within the lesion and the fibrous cap. no significant differences in any of the indices of stability examined, including collagen content of the lesion and fibrous cap.

Taken together, these data suggest that, in the absence of SMC investment, mesenchymal transitions of non-SMC-derived cells are capable of only temporarily maintaining indices of lesion stability. (Newman et al., 2021)

6

Conclusion & Outlook

We are closer to doing postGWAS analyses, we really hope that the database makes everything smoother. And we have a system where we can functionally access these identified SNPs. We are close to a point where we can combine both parts of the project.

integration of Ensembl database

Abkürzungsverzeichnis

A adenin
AF488 Alexa Fluor® 488
bp basepairs
C cytosin
DNA deoxyribonucleic acid
dsDNA doublestranded DNA
E. coli *Escherichia coli*
EDTA Ethylenediaminetetraacetic acid
G guanine
HCl hydrogen chloride
qPCR quantative polymerase chain reaction
T thymin
HAoSMC human aortic smooth muscle cell
IF immunofluorescence
TGF β Transforming Growth Factor beta
SMGS Smooth Muscle Cell Growth Supplement
IL-1 Interleukin 1 beta
PDGF-BB platelet-derived growth factor-BB
TGF β Transforming Growth Factor beta
DE Deutschland
MMP9 Matrix metalloproteinase 9
CNN1 Calponin 1
GAPDH Glyceraldehyde-3-phosphate dehydrogenase
col I collagen type I
OCR oxygen consumption rate
ECAR extracellular acidification rate
FCCP Carbonyl cyanide-p-trifluoromethoxyphenylhydrazone
CAD coronary artery disease
PBS phosphate buffered solution
FBS fetal bovine serum
Cq quantification cycle
RNA ribonucleic acid
RT reverse transcription
DTT dithiothreitol
dNTP deoxyribose nucleoside triphosphate
ROS reactive oxygen species
NAC N-acetylcystein
cCRE candidate cis regulatory elements
LD lipid disequilibrium

GWAS genome wide association study

L2G link to gene

H₂O₂ hydrogen peroxide

O₂^{·-} superoxide anion radical

O₂ elemental oxygen

MI myocardial infarction

VSMC vascular smooth muscle cell

KLF4 Kruppel-like factor 4

TF transcription factor

PDGFR Platelet-derived growth factor receptor

MAP mitogen activated protein

STAT signal transducers and activators of transcription

PI3K phosphatidylinositol 3'-kinase

ROS reactive oxygen species

Bibliography

Disease Control and Prevention, Centers for (2022). *Heart Disease Facts / Cdc.Gov*. Centers for Disease Control and Prevention. URL: <https://www.cdc.gov/heartdisease/facts.htm> (visited on 06/07/2022).

Fryar, Cheryl D (2012). Prevalence of Uncontrolled Risk Factors for Cardiovascular Disease: United States, 1999–2010, 8.

National Health Service (24 Oct 2017, 4:45 p.m.). *Heart Attack*. URL: <https://www.nhs.uk/conditions/heart-attack/> (visited on 06/07/2022).

Task Force Members et al. (2013). 2013 ESC Guidelines on the Management of Stable Coronary Artery Disease: The Task Force on the Management of Stable Coronary Artery Disease of the European Society of Cardiology. *European Heart Journal* *34*, 2949–3003. DOI: [10.1093/eurheartj/ehs296](https://doi.org/10.1093/eurheartj/ehs296).

Tucker, William D., Arora, Yingyot, and Mahajan, Kunal (2022). 1. 1, Treasure Island (FL): StatPearls Publishing.

Yap, Carmen et al. (2021). Six Shades of Vascular Smooth Muscle Cells Illuminated by KLF4 (Krüppel-Like Factor 4). *Arteriosclerosis, Thrombosis, and Vascular Biology*, ATVBAHA121316600. DOI: [10.1161/ATVBAHA.121.316600](https://doi.org/10.1161/ATVBAHA.121.316600).

Grootaert, Mandy O J and Bennett, Martin R (2021). Vascular Smooth Muscle Cells in Atherosclerosis: Time for a Re-Assessment. *Cardiovascular Research* *117*, 2326–2339. DOI: [10.1093/cvr/cvab046](https://doi.org/10.1093/cvr/cvab046).

Goumans, Marie-José and Dijke, Peter ten (2018). TGF- Signaling in Control of Cardiovascular Function. *Cold Spring Harbor Perspectives in Biology* *10*, a022210. DOI: [10.1101/cshperspect.a022210](https://doi.org/10.1101/cshperspect.a022210).

Batlle, Eduard and Massagué, Joan (2019). Transforming Growth Factor- Signaling in Immunity and Cancer. *Immunity* *50*, 924–940. DOI: [10.1016/j.immuni.2019.03.024](https://doi.org/10.1016/j.immuni.2019.03.024).

Davis-Dusenbery, Brandi N. et al. (2011). Down-Regulation of Krüppel-like Factor-4 (KLF4) by MicroRNA-143/145 Is Critical for Modulation of Vascular Smooth Muscle Cell Phenotype by Transforming Growth Factor- and Bone Morphogenetic Protein 4. *The Journal of Biological Chemistry* *286*, 28097–28110. DOI: [10.1074/jbc.M111.236950](https://doi.org/10.1074/jbc.M111.236950).

Takahashi, Kazutoshi et al. (2007). Induction of Pluripotent Stem Cells from Adult Human Fibroblasts by Defined Factors. *Cell* *131*, 861–872. DOI: [10.1016/j.cell.2007.11.019](https://doi.org/10.1016/j.cell.2007.11.019).

- Pan, Huize et al. (2020). Single-Cell Genomics Reveals a Novel Cell State During Smooth Muscle Cell Phenotypic Switching and Potential Therapeutic Targets for Atherosclerosis in Mouse and Human. *Circulation* *142*, 2060–2075. DOI: [10.1161/CIRCULATIONAHA.120.048378](https://doi.org/10.1161/CIRCULATIONAHA.120.048378).
- Chen, Po-Han, Chen, Xiaoyan, and He, Xiaolin (2013). Platelet-Derived Growth Factors and Their Receptors: Structural and Functional Perspectives. *Biochimica et biophysica acta* *1834*, 2176–2186. DOI: [10.1016/j.bbapap.2012.10.015](https://doi.org/10.1016/j.bbapap.2012.10.015).
- Heldin, Carl-Henrik (2013). Targeting the PDGF Signaling Pathway in Tumor Treatment. *Cell Communication and Signaling* *11*, 97. DOI: [10.1186/1478-811X-11-97](https://doi.org/10.1186/1478-811X-11-97).
- Hu, Weining and Huang, Yu (2015). Targeting the Platelet-Derived Growth Factor Signalling in Cardiovascular Disease. *Clinical and Experimental Pharmacology and Physiology* *42*, 1221–1224. DOI: [10.1111/1440-1681.12478](https://doi.org/10.1111/1440-1681.12478).
- Andrae, Johanna, Gallini, Radosa, and Betsholtz, Christer (2008). Role of Platelet-Derived Growth Factors in Physiology and Medicine. *Genes & Development* *22*, 1276–1312. DOI: [10.1101/gad.1653708](https://doi.org/10.1101/gad.1653708).
- Levéen, P. et al. (1994). Mice Deficient for PDGF B Show Renal, Cardiovascular, and Hematological Abnormalities. *Genes & Development* *8*, 1875–1887. DOI: [10.1101/gad.8.16.1875](https://doi.org/10.1101/gad.8.16.1875).
- Robson, M. C. et al. (1992). Platelet-Derived Growth Factor BB for the Treatment of Chronic Pressure Ulcers. *Lancet (London, England)* *339*, 23–25. DOI: [10.1016/0140-6736\(92\)90143-q](https://doi.org/10.1016/0140-6736(92)90143-q).
- Raines, Elaine W (2004). PDGF and Cardiovascular Disease. *Cytokine & growth factor reviews* *15*, 237–254. DOI: [10.1016/j.cytogfr.2004.03.004](https://doi.org/10.1016/j.cytogfr.2004.03.004).
- He, Chaoyong et al. (2015). PDGFR Signalling Regulates Local Inflammation and Synergizes with Hypercholesterolaemia to Promote Atherosclerosis. *Nature Communications* *6* (1), 7770. DOI: [10.1038/ncomms8770](https://doi.org/10.1038/ncomms8770).
- Newman, Alexandra A. C. et al. (2021). Multiple Cell Types Contribute to the Atherosclerotic Lesion Fibrous Cap by PDGFR and Bioenergetic Mechanisms. *Nature Metabolism* *3* (2), 166–181. DOI: [10.1038/s42255-020-00338-8](https://doi.org/10.1038/s42255-020-00338-8).
- Sies, Helmut and Jones, Dean P. (2020). Reactive Oxygen Species (ROS) as Pleiotropic Physiological Signalling Agents. *Nature Reviews Molecular Cell Biology* *21* (7), 363–383. DOI: [10.1038/s41580-020-0230-3](https://doi.org/10.1038/s41580-020-0230-3).
- Sundaresan, M. et al. (1995). Requirement for Generation of H₂O₂ for Platelet-Derived Growth Factor Signal Transduction. *Science (New York, N.Y.)* *270*, 296–299. DOI: [10.1126/science.270.5234.296](https://doi.org/10.1126/science.270.5234.296).

- Bouzigues, Cedric I. et al. (2014). Regulation of the ROS Response Dynamics and Organization to PDGF Motile Stimuli Revealed by Single Nanoparticle Imaging. *Chemistry & Biology* 21, 647–656. DOI: [10.1016/j.chembiol.2014.02.020](https://doi.org/10.1016/j.chembiol.2014.02.020).
- Uffelmann, Emil et al. (2021). Genome-Wide Association Studies. *Nature Reviews Methods Primers* 1 (1), 1–21. DOI: [10.1038/s43586-021-00056-9](https://doi.org/10.1038/s43586-021-00056-9).
- Flint, Jonathan (2013). GWAS. *Current Biology* 23, R265–R266. DOI: [10.1016/j.cub.2013.01.040](https://doi.org/10.1016/j.cub.2013.01.040).
- Schaid, Daniel J., Chen, Wenan, and Larson, Nicholas B. (2018). From Genome-Wide Associations to Candidate Causal Variants by Statistical Fine-Mapping. *Nature reviews. Genetics* 19, 491–504. DOI: [10.1038/s41576-018-0016-z](https://doi.org/10.1038/s41576-018-0016-z).
- Lichou, Florence and Trynka, Gosia (2020). Functional Studies of GWAS Variants Are Gaining Momentum. *Nature Communications* 11, 6283. DOI: [10.1038/s41467-020-20188-y](https://doi.org/10.1038/s41467-020-20188-y).
- Slatkin, Montgomery (2008). Linkage Disequilibrium — Understanding the Evolutionary Past and Mapping the Medical Future. *Nature reviews. Genetics* 9, 477–485. DOI: [10.1038/nrg2361](https://doi.org/10.1038/nrg2361).
- Mountjoy, Edward et al. (2021). An Open Approach to Systematically Prioritize Causal Variants and Genes at All Published Human GWAS Trait-Associated Loci. *Nature Genetics* 53 (11), 1527–1533. DOI: [10.1038/s41588-021-00945-5](https://doi.org/10.1038/s41588-021-00945-5).
- Zerbino, Daniel R. et al. (2015). The Ensembl Regulatory Build. *Genome Biology* 16, 56. DOI: [10.1186/s13059-015-0621-5](https://doi.org/10.1186/s13059-015-0621-5).
- SCREEN: Search Candidate Regulatory Elements by ENCODE* (n.d.). URL: <https://screen.encodeproject.org/> (visited on 06/07/2022).
- Moore, Jill E. et al. (2020). Expanded Encyclopaedias of DNA Elements in the Human and Mouse Genomes. *Nature* 583 (7818), 699–710. DOI: [10.1038/s41586-020-2493-4](https://doi.org/10.1038/s41586-020-2493-4).
- Buenrostro, Jason D. et al. (2013). Transposition of Native Chromatin for Fast and Sensitive Epigenomic Profiling of Open Chromatin, DNA-binding Proteins and Nucleosome Position. *Nature Methods* 10 (12), 1213–1218. DOI: [10.1038/nmeth.2688](https://doi.org/10.1038/nmeth.2688).
- Buenrostro, Jason D. et al. (2015a). ATAC-seq: A Method for Assaying Chromatin Accessibility Genome-Wide. *Current Protocols in Molecular Biology* 109, 21.29.1–21.29.9. DOI: [10.1002/0471142727.mb2129s109](https://doi.org/10.1002/0471142727.mb2129s109).
- Buenrostro, Jason D. et al. (2015b). Single-Cell Chromatin Accessibility Reveals Principles of Regulatory Variation. *Nature* 523 (7561), 486–490. DOI: [10.1038/nature14590](https://doi.org/10.1038/nature14590).
- Fulco, Charles P. et al. (2019). Activity-by-Contact Model of Enhancer–Promoter Regulation from Thousands of CRISPR Perturbations. *Nature Genetics* 51 (12), 1664–1669. DOI: [10.1038/s41588-019-0538-0](https://doi.org/10.1038/s41588-019-0538-0).

- Nasser, Joseph et al. (2021). Genome-Wide Enhancer Maps Link Risk Variants to Disease Genes. *Nature* *593* (7858), 238–243. DOI: [10.1038/s41586-021-03446-x](https://doi.org/10.1038/s41586-021-03446-x).
- Lieberman-Aiden, Erez et al. (2009). Comprehensive Mapping of Long-Range Interactions Reveals Folding Principles of the Human Genome. *Science* *326*, 289–293. DOI: [10.1126/science.1181369](https://doi.org/10.1126/science.1181369).
- Wit, Elzo de and Laat, Wouter de (2012). A Decade of 3C Technologies: Insights into Nuclear Organization. *Genes & Development* *26*, 11–24. DOI: [10.1101/gad.179804.111](https://doi.org/10.1101/gad.179804.111).
- Dixon, Jesse R. et al. (2012). Topological Domains in Mammalian Genomes Identified by Analysis of Chromatin Interactions. *Nature* *485* (7398), 376–380. DOI: [10.1038/nature11082](https://doi.org/10.1038/nature11082).
- Wang, Yanli et al. (2018b). The 3D Genome Browser: A Web-Based Browser for Visualizing 3D Genome Organization and Long-Range Chromatin Interactions. *Genome Biology* *19*, 151. DOI: [10.1186/s13059-018-1519-9](https://doi.org/10.1186/s13059-018-1519-9).
- Pombo, Ana and Dillon, Niall (2015). Three-Dimensional Genome Architecture: Players and Mechanisms. *Nature Reviews Molecular Cell Biology* *16* (4), 245–257. DOI: [10.1038/nrm3965](https://doi.org/10.1038/nrm3965).
- Burtenshaw, Denise et al. (2019). Reactive Oxygen Species (ROS), Intimal Thickening, and Subclinical Atherosclerotic Disease. *Frontiers in Cardiovascular Medicine* *6*, 89. DOI: [10.3389/fcvm.2019.00089](https://doi.org/10.3389/fcvm.2019.00089).
- Huggett, Jim and Bustin, Stephen A. (2011). Standardisation and Reporting for Nucleic Acid Quantification. *Accreditation and Quality Assurance* *16*, 399. DOI: [10.1007/s00769-011-0769-y](https://doi.org/10.1007/s00769-011-0769-y).
- Tipney, Hannah and Hunter, Lawrence (2010). An Introduction to Effective Use of Enrichment Analysis Software. *Human Genomics* *4*, 202. DOI: [10.1186/1479-7364-4-3-202](https://doi.org/10.1186/1479-7364-4-3-202).
- Lee, Hyun Jung et al. (2007). The Role of STAT1/IRF-1 on Synergistic ROS Production and Loss of Mitochondrial Transmembrane Potential during Hepatic Cell Death Induced by LPS/d-GalN. *Journal of Molecular Biology* *369*, 967–984. DOI: [10.1016/j.jmb.2007.03.072](https://doi.org/10.1016/j.jmb.2007.03.072).
- Wang, Yan et al. (2018a). The STAT-ROS Cycle Extends IFN-induced Cancer Cell Apoptosis. *International Journal of Oncology* *52*, 305–313. DOI: [10.3892/ijo.2017.4196](https://doi.org/10.3892/ijo.2017.4196).
- Harman, Jennifer L. and Jørgensen, Helle F. (2019). The Role of Smooth Muscle Cells in Plaque Stability: Therapeutic Targeting Potential. *British Journal of Pharmacology* *176*, 3741–3753. DOI: [10.1111/bph.14779](https://doi.org/10.1111/bph.14779).
- Alexander, Matthew R. and Owens, Gary K. (2012). Epigenetic Control of Smooth Muscle Cell Differentiation and Phenotypic Switching in Vascular Development and Disease. *Annual Review of Physiology* *74*, 13–40. DOI: [10.1146/annurev-physiol-012110-142315](https://doi.org/10.1146/annurev-physiol-012110-142315).